SUPERSONIC WIND TUNNEL

TESTS OF TWO ROCKET PROPELLED PROJECTILE MODELS

Thesis by

Mike Fossier

and

John Small

In Partial Fulfillment of the Requirements for the Professional Degree in Aeronautical Engineering

California Institute of Technology

Pasadena, California

-1947-

Acknowledgements

The authors wish to express their thanks to Allen Puckett, who was the originator and supervisor of the project.

They would also like to express their thanks to the staff of the GALCIT supersonic wind tunnel, and especially to Richard Schamberg, whose assistance and encouragement were invaluable to the completion of the project.

Table of Contents

Section	Title	Page
I	Summary	1
II	Description of Apparatus	2
III	Static Calibration of Balances	7
IV	Model Testing Procedure	12
V	Determination of the Tare Forces	24
VI	Determination of Maximum Model Sizr	28
VII	Test Results and Analysis	32

I. Summary

Two models of rocket propelled projectiles have been tested in the Galcit 2½ inch supersonic wind tunnel at a Mach Number of 3.06, and angles of attack from 0° to 10°. Variations of lift, drag, pitching moment, and position of center of pressure with angle of attack have been obtained for each model.

A strain gage balance system, which was designed to measure the forces acting on the models, was found to be entirely satisfactory for this purpose.

The results were found to agree very closely with the small perturbation theory for supersonic flow.

II. Description of Apparatus

The tests were conducted in the GALCIT supersonic wind tunnel, which has a test section $2\frac{1}{2}$ inches square. Photographs of the test section and nozzle blocks with model in place are shown in figure 2-1. A complete description of the wind tunnel may be found in the Final Report - Galcit Supersonic Wind Tunnel Projectile Tests Contract W-101 ORD-1312 (741) .

Forces on the model support strut are measured through the balance linkage shown in figure 2-3 by a set of strain gages attached to the horizontal balance members. The strain gage deflections are recorded by a Brown potentiometer.

Figure 2-2 shows the panel board of the Brown potentiometer.

In order to determine the numerical relationships between the readings of the Brown potentiometer and the aerodynamic forces transmitted to the model support strut by the model, a set of static calibration devices was designed.

The drag calibrator, shown in figures 2-4 and 2-5, was designed to minimize friction by transferring the forces through a set of knife edges and seats to the support strut.

The lift calibrator, shown in figures 2-6 and 2-7, consists of a lift pan assembly acting through a pivot point on either of two stinger attachments. The short stinger attachment may be adjusted so as to apply the load at a point directly over the axis of the vertical member of the L_2 balance. Thus no load is transmitted to the L_1 balance. The other attachment applies the load at a much longer distance from the trunnion axis in order to obtain a sizeable load on the L_1 balance.

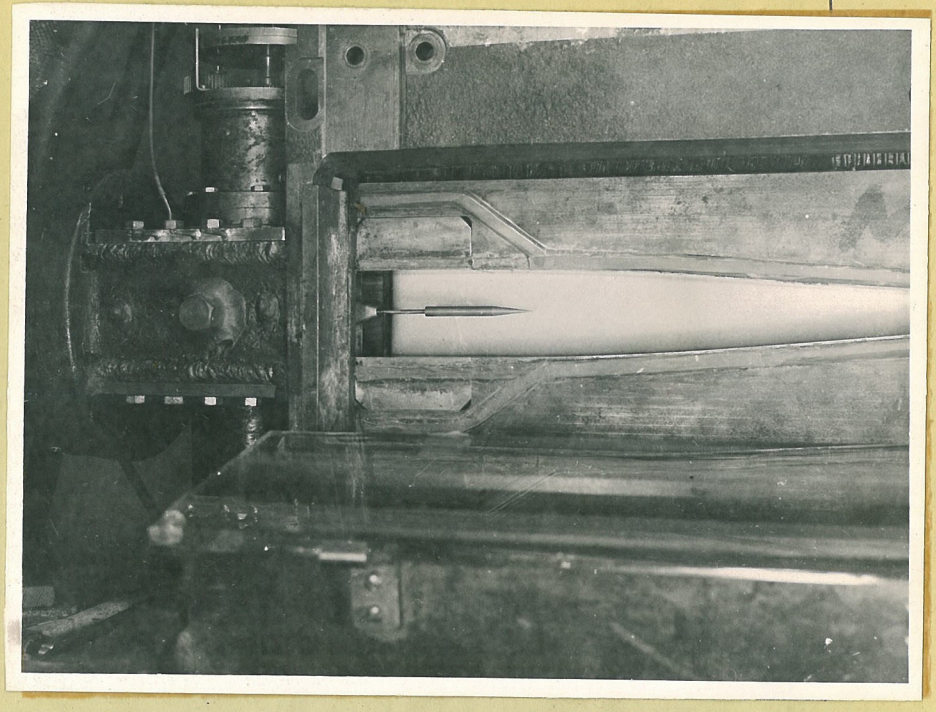

Figure 2-1

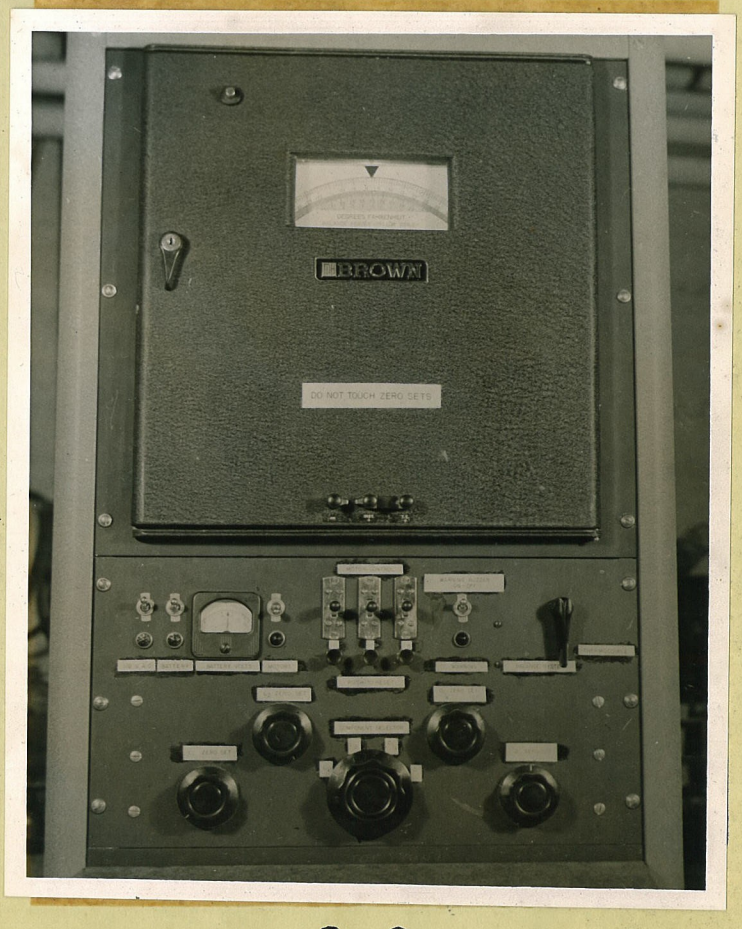

Figure 2-2

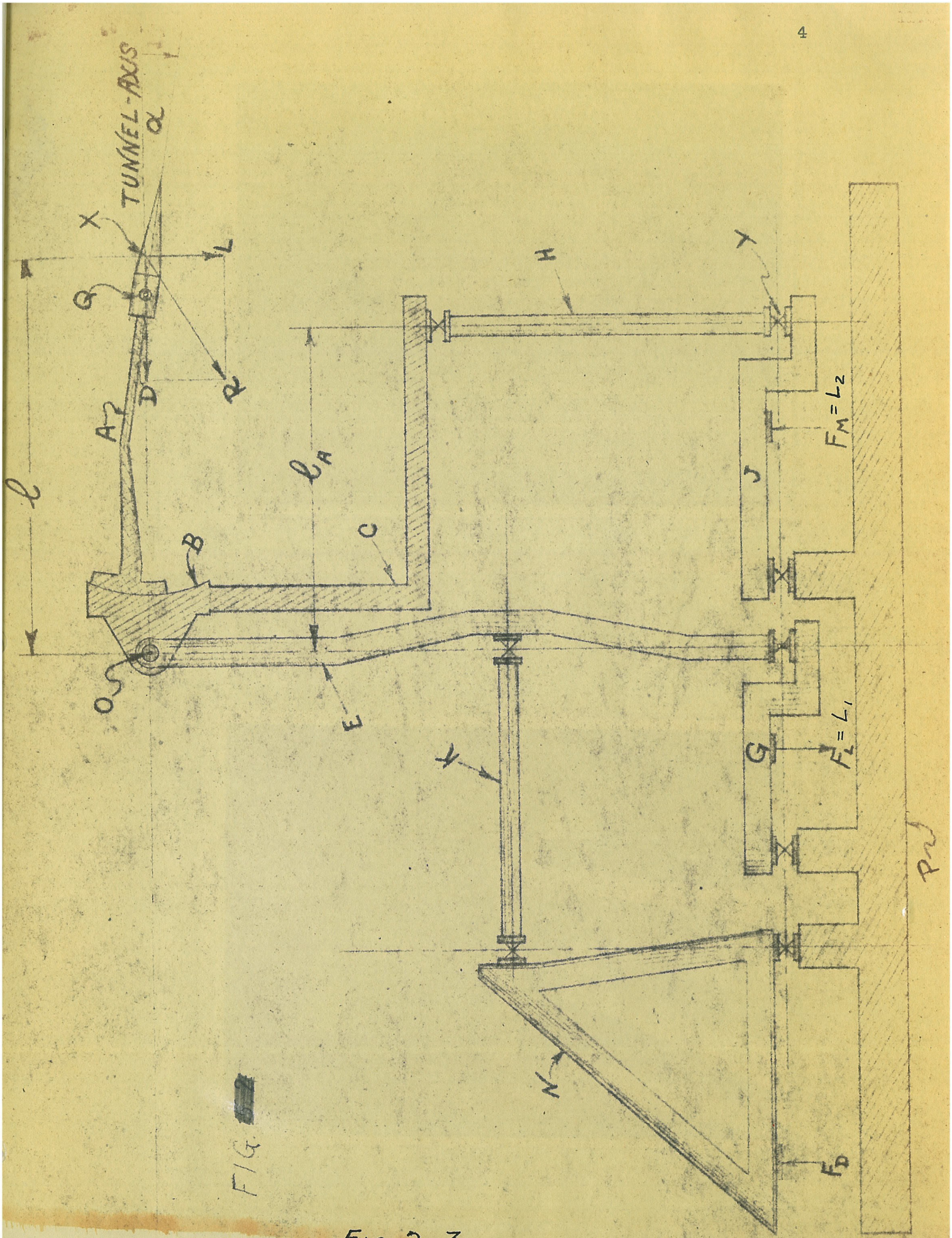

FIG. 2-3

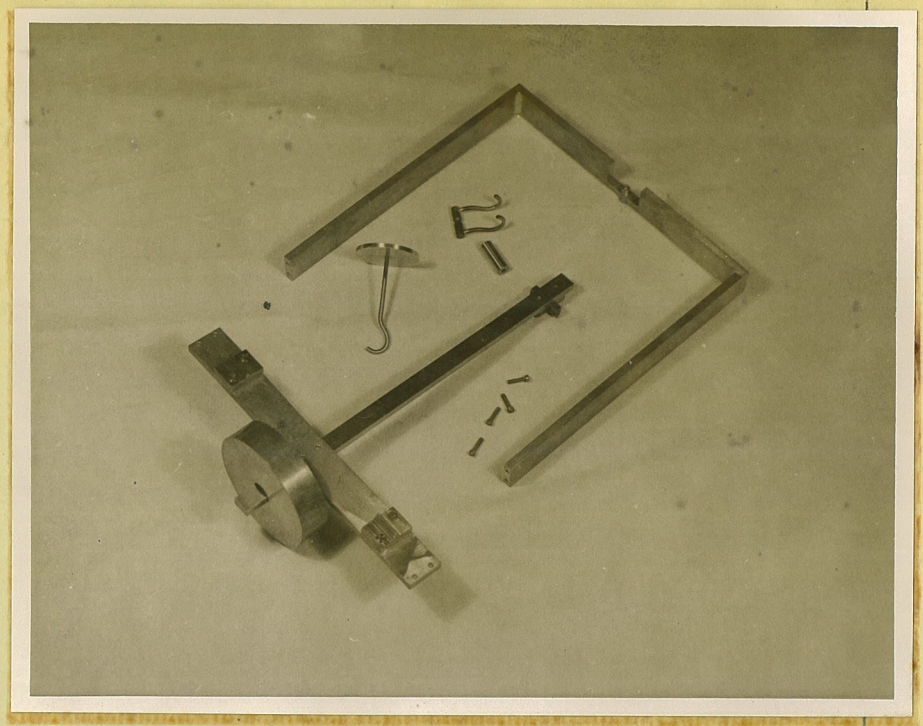

Figure 2-4

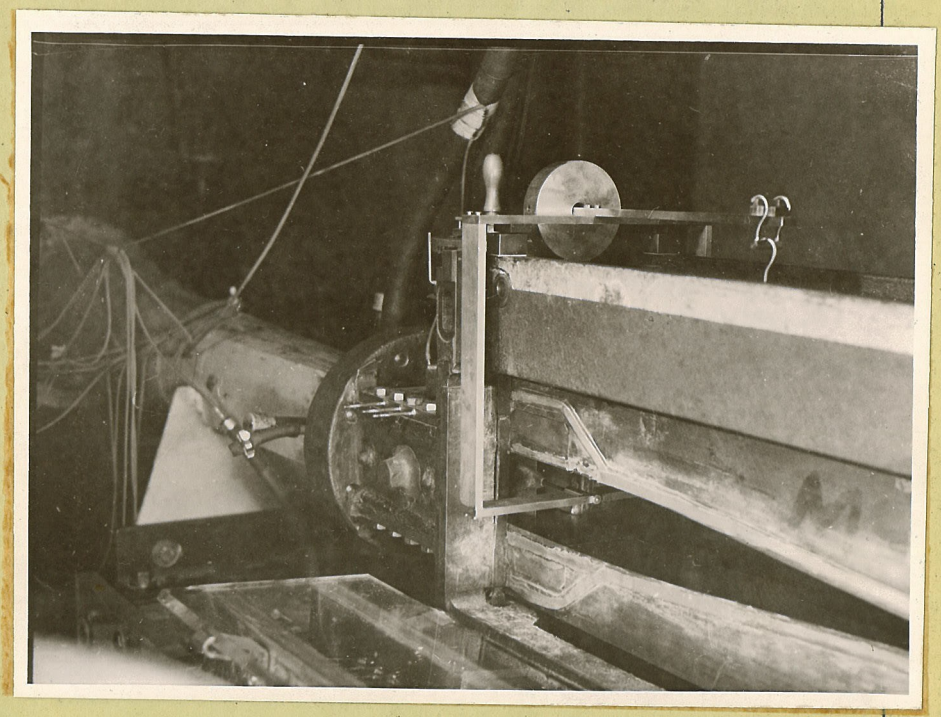

Figure 2-5

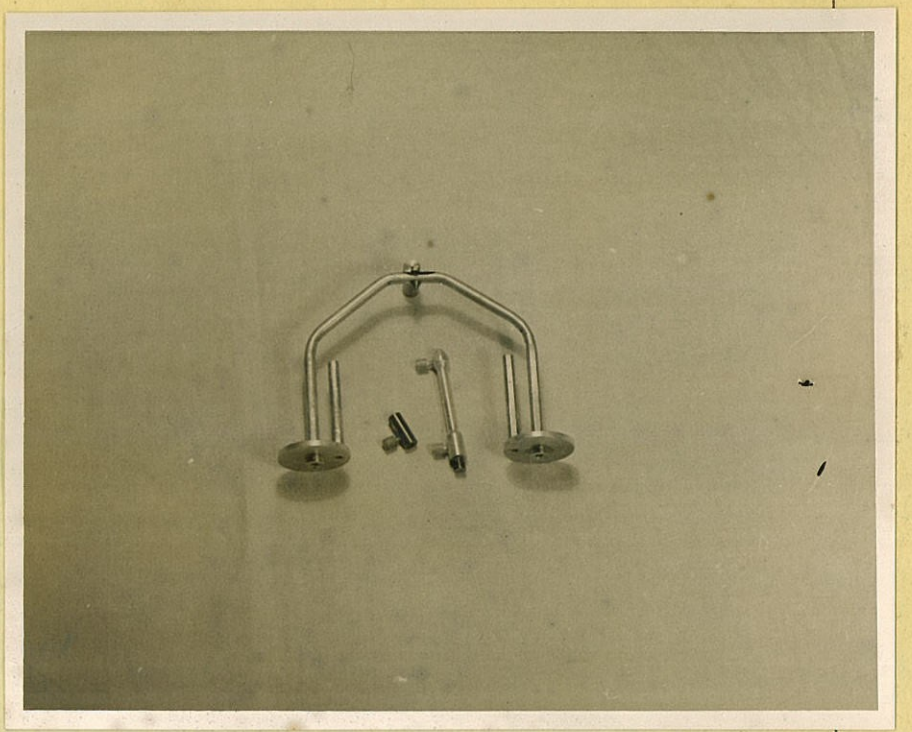

Figure 2-6

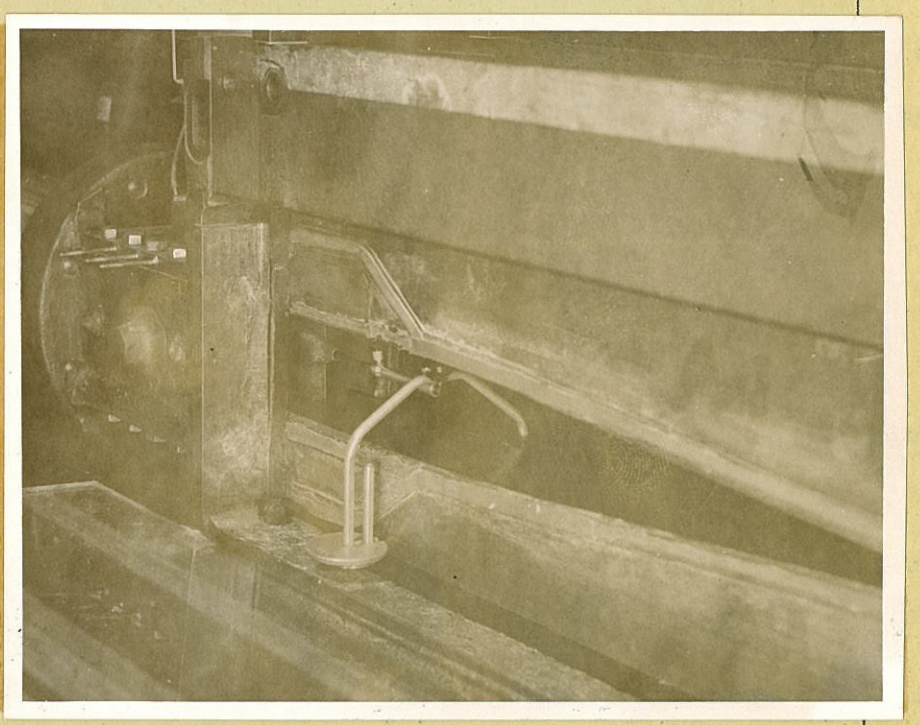

Figure 2-7

III. Static Calibration of Balance

As can be seen from a study of the balance linkage system (figure 2-3), the forces measured by the balance, corresponding to the forces F_D, F_L, and F_M, will be:

$$\text{Drag} = D = \delta N_D = \delta_{\frac{1}{4}} N_{D_{\frac{1}{4}}} \tag{3.1}$$

$$\text{Lift} = L = \lambda_1 N_{L_1} + \lambda_2 N_{L_2} \tag{3.2}$$

$$\text{Moment about trunnion axis} = M_o = \mu N_{L_2} \tag{3.3}$$

where N_D, $N_{D_{\frac{1}{4}}}$, N_{L_1}, and N_{L_2} are readings of the potentiometer. $N_{D_{\frac{1}{4}}}$ represents the reading of the potentiometer in which the scale has been magnified electrically four times over the N_D scale.

The constants δ, $\delta_{\frac{1}{4}}$, λ_1, λ_2, and μ depend on the ratios of the lengths of the various balance links, the constants in the electrical system, and the strain gages. The values of these constants were determined by a direct static calibration.

The drag calibration was performed, as shown in figure 2-5, by transferring a known vertical force into the drag direction through a set of frictionless knife edges.

The lift and moment calibrations were performed, as shown in figure 2-7, by suspending weights from the calibrating attachment on the model support strut. The distance "ℓ" (see Figure 2-3) from the point of application of the lift forces to the trunnion axis of the balance is adjustable.

The calibration curves deviated somewhat from a straight line, and their slopes were determined so as to give the minimum percentage error over the complete range of each component. This was done by the method of Least Squares:

Let y_i represent the reading corresponding to a particular applied load, x_i. Then if K is the slope,

$$\sum_{i=1}^{n} \left(\frac{y_i - K x_i}{y_i} \right)^2 = \text{minimum}$$

$$= \sum_{i=1}^{n} \left(1 - \frac{x_i}{y_i} K \right)^2 = \sum_{i=1}^{n} \left(1 - 2 \frac{x_i}{y_i} K + \left(\frac{x_i}{y_i} \right)^2 K^2 \right).$$

Setting $\frac{\partial}{\partial K}$ of this equal to zero we have:

or
$$-2 \sum_{i=1}^{n} \frac{x_i}{y_i} + 2K \sum_{i=1}^{n} \left(\frac{x_i}{y_i} \right)^2 = 0$$

$$K = \frac{\sum_{i=1}^{n} \left(\frac{x_i}{y_i} \right)}{\sum_{i=1}^{n} \left(\frac{x_i}{y_i} \right)^2} . \tag{3.4}$$

Rewriting equations (3.2) and (3.3) in terms of increments of the lift load, ΔL, moment, ΔM_o, and potentiometer readings, ΔN_{L_1}, and ΔN_{L_2}, gives

$$\Delta L = \lambda_1 \Delta N_{L_1} + \lambda_2 \Delta N_{L_2} \tag{3.5}$$

$$\Delta M_o = \eta \Delta N_{L_2} = \ell \Delta L \tag{3.6}$$

From equation (3.6),

$$\eta = \ell \times \frac{\Delta L}{\Delta N_{L_2}} = \ell \frac{dL}{d N_{L_2}} , \tag{3.7}$$

where the slope $\left(\frac{dL}{d N_{L_2}} \right)$ is determined from the static calibration by the method outlined above for a particular measured value of the distance "ℓ".

It can be seen from figure 2-3 that for the special value of $\ell = \ell_A$, such that the point of application of the load lies directly above the

axis of the vertical member of the L_2 balance, the entire lift force is accounted for by the L_2 strain gage, so that $(\Delta N_{L_1})_A = 0$. This point is determined experimentally by changing the point of application of the load until $\Delta N_{L_1} = 0$.

Hence, from equations (3.5) and (3.7)

$$\lambda_2 = \frac{(\Delta L)_A}{(\Delta N_{L_2})_A} = \left(\frac{dL}{dN_{L_2}}\right)_A = \frac{\mu}{\ell_A} . \tag{3.8}$$

If the distance ℓ be changed to some other value, say $\ell = \ell_B \neq \ell_A$, then from equations (3.5) and (3.7)

$$(\Delta L)_B = \lambda_{L_1}(\Delta N_{L_1})_B + \lambda_{L_2}\frac{\ell_B}{\mu}(\Delta L)_B ,$$

or

$$\lambda_{L_1} = \left(1 - \frac{\lambda_{L_2}\ell_B}{\mu}\right) \times \frac{(\Delta L)_B}{(\Delta N_{L_1})_B} ,$$

and finally from equation (3.8)

$$\lambda_{L_1} = \left(1 - \frac{\ell_B}{\ell_A}\right)\left(\frac{dL}{dN_{L_1}}\right)_B . \tag{3.9}$$

After determination of the calibration constant, a check of these values was made by again applying static loads. The values of the applied loads indicated by the Potentiometer and the calibration constants were compared with the known values of the applied weights and arbitrary length "ℓ".

The results of the static calibration are tabulated in table 3.1.

The results of a typical drag static check run are plotted in figure 3-1, showing per cent error as a function of per cent of maximum load. This shows the maximum error to be within 1% of the load throughout the load range.

$D_{\frac{1}{4}} = .003834 \times N_{D_{\frac{1}{4}}}$	(LB)
$D_1 = .01561 \times N_{D_1}$	(LB)
$L = .010858 \times N_{L_1} + .018002 \times N_{L_2}$	(LB)
$M_o = .12422 \times N_{L_2}$	(IN-LB)

Table 3.1

Results of Static Calibration

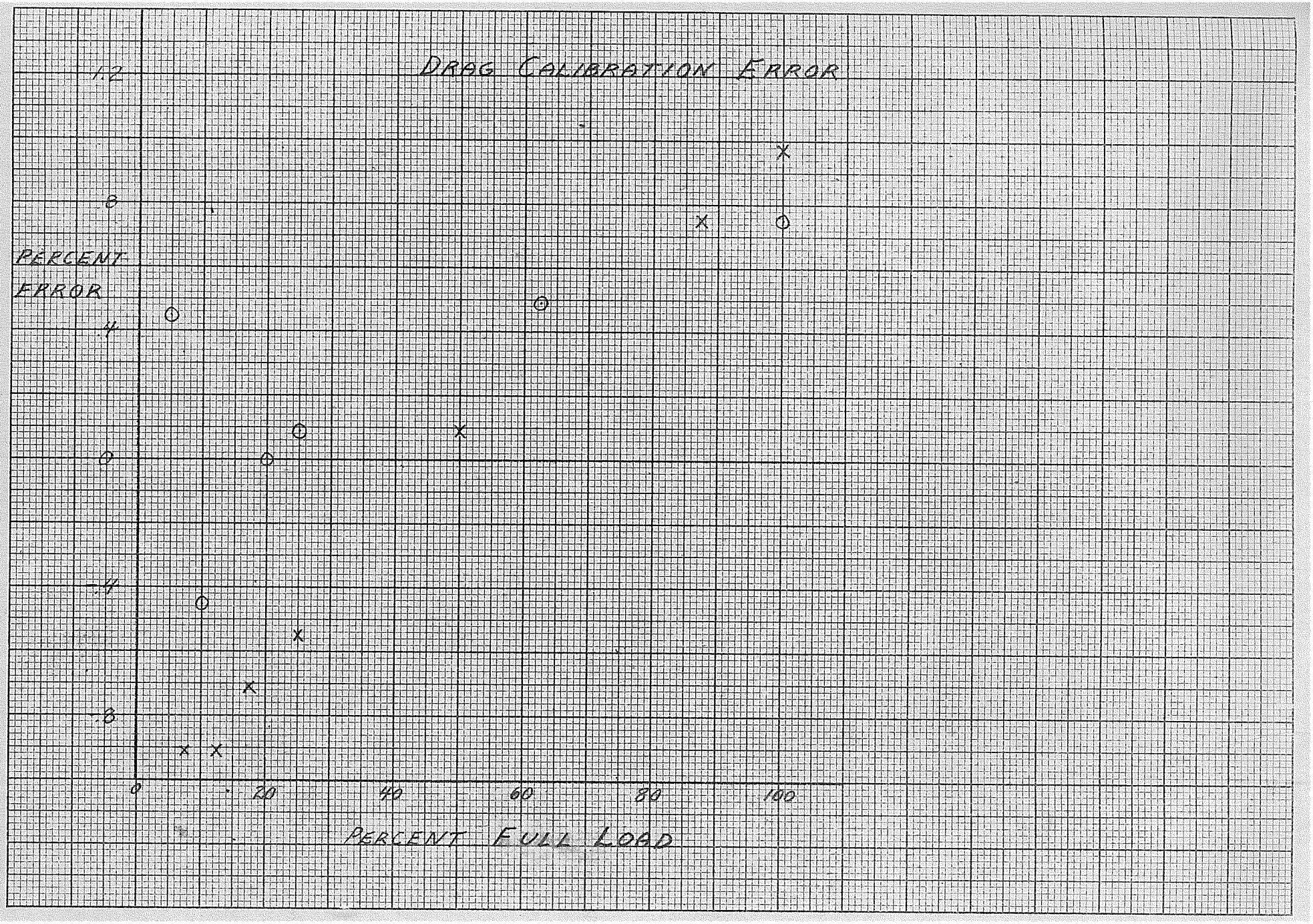
DRAG CALIBRATION ERROR
1.2
.8
PERCENT
ERROR
.4
0
-.4
-.8
0
20
40
60
80
100
PERCENT FULL LOAD

FIG 3-1

IV. Model Testing Procedure

1. Determination of the balance tank pressure

The balance system is located in an airtight metal tank. The tank is open to the tunnel through the small opening in the windshield through which the model support strut also goes. For values of the balance tank pressure, p_{bt}, less than $(p_{bt})_{crit}$ air flows from the test section into the windshield opening ("inflow"), whereas for values of p_{bt} greater than $(p_{bt})_{crit}$ there is a flow of air from the windshield into the test section ("outflow"). The pressure inside the balance tank may be reduced below $(p_{bt})_{crit}$ by means of an auxiliary vacuum pump. p_{bt} may be raised above $(p_{bt})_{crit}$ by allowing a controllable amount of air to flow from the atmosphere into the balance tank.

For drag measurements the best results are obtained with the "inflow"[1] condition. This produces drag tare forces small compared to the drag of the model and independent of small variations in p_{bt}.

However, the smallest lift and moment tare forces are obtained when there is a small amount of air flow out of the windshield.

Hence, it is seen that for simplicity of operation, separate runs should be made for drag and for lift and moment measurements.

2. Routine Testing Procedure

a) The model to be tested is screwed to the support strut. The distance, t, from the model base to the trunnion axis is determined by measuring the distance from the model base to a known scribe mark on the strut.

1 Puckett, A. E., and Schamberg, R., Final Report - GALCIT Supersonic Wind Tunnel Projectile Tests, Contract W-101 ORD-1312 (741), Page 22.

b) The model support strut is aligned to zero angle of attack, after which the wind tunnel windows are closed.

c) The Brown potentiometer is set at zero for the force components to be measured.

d) The wind tunnel compressor is started.

e) For drag runs, the auxiliary vacuum pump is started, and the balance tank pressure adjusted for the optimum "inflow" condition by means of a throttling valve.

For lift runs, the balance tank pressure is adjusted for the optimum "outflow" condition by means of an air bleed valve.

f) When steady supersonic flow conditions have been established, a Schlieren photograph of the flow about the model is taken.

g) The value of the Brown reading is recorded.

h) Simultaneously with g), the following pressures are recorded:

1) Barometric pressure on standard mercury manometer.

2) Wind tunnel supply gage pressure, p_o, measured on a Bourdon gage.

3) Pressure difference $(p_{bt} - p_{mb})$ between balance tank and model base measured on tetra - bromo - ethane U tube manometer on drag runs and on mercury multiple manometer on both lift and drag runs.

4) Pressure difference $(p_4 - p_{mb})$ between a standard pressure at the test section wall (p_4) and the base of the model, p_{mb}, measured on tetra - bromo- ethane and mercury manometers.

i) The angle of attack is changed without stopping the airflow, and steps g) and h) are repeated for each angle of attack.

j) Schlieren photographs are taken at points of interest.

3. Data Reduction

The aerodynamic force data are presented in terms of dimensionless coefficients. The drag, lift, and moment coefficients generally used in aerodynamics are defined by equations (4.1), (4.2), and (4.3), respectively.

$$C_D = \frac{D}{\frac{\rho}{2} u^2 A} \tag{4.1}$$

$$C_L = \frac{L}{\frac{\rho}{2} u^2 A} \tag{4.2}$$

$$C_M = \frac{M}{\frac{\rho}{2} u^2 A d} \tag{4.3}$$

where d is the basic diameter or caliber of the projectile, and A is the area of the model base, $\frac{\pi}{4} d^2$.

The product $\frac{\rho}{2} u^2$, where ρ is the air density and u the relative velocity, may be written as $\left(\frac{q_t}{p_o}\right) p_o$, where q_t is the dynamic pressure in the test section, and p_o is the wind tunnel supply pressure. (q_t / p_o) is a function of the test section Mach number, M_t, only, namely:

$$\frac{q_t}{p_o} = \frac{1}{2} \gamma \left(\frac{p_s}{p_o}\right) M_t^2 = \frac{1}{2} \gamma M_t^2 \left(1 + \frac{\gamma - 1}{2} M_t^2\right)^{-\frac{\gamma}{\gamma - 1}}, \tag{4.4}$$

where p_s is the test section free stream static pressure and $\gamma = 1.400$.

The reduction of drag, lift, moment, and base pressure data will now be discussed individually.

a) Drag data reduction.

From equation (3.1), it follows that the drag force measured by the balance is given by:

$$D_{1_b} = 0.01561 \times N_{D_1} \quad (LB.) \tag{4.5}$$

or

$$D_{\frac{1}{4}_b} = 0.003834 \times N_{D_{\frac{1}{4}}} \quad (LB.) \, .$$

As can be seen from figure 4-1 this value must be corrected for the so-called "Piston effect", ΔD, due to the difference between the model base pressure, p_{mb}, and the balance tank pressure, p_{bt}. That is,

$$\Delta D = \frac{\pi}{4} d_{ST}^2 \left(P_{bt} - P_{mb} \right) \, , \tag{4.6}$$

where d_{ST} is the stinger diameter.

The true drag of the model itself is given by:

$$D = \left(D_b + \Delta D \right) - D_T = D' - D_T \, , \tag{4.7}$$

where D_T is the tare drag on the model support structure not accounted for in the piston effect. It is convenient to reduce this equation to coefficient form

$$C_D = C_D' - C_{D_T} \, , \tag{4.8}$$

where C_D' is calculated from

$$C_D' = \frac{D'}{\left(\frac{q_\infty}{P_o} \right) P_o A} \, , \tag{4.9}$$

and the tare coefficient C_{D_T} is a known function of the Mach Number, M, the indicated angle of attack, α_i , and the model diameter, d.

The method of determining C_{D_T} is described in section V.

It is usually convenient to reduce the drag to the so-called "fore-drag". This is the drag which the projectile would experience if the pressure at the base of the model were equal to free stream static pressure. The "fore drag" is useful because it is defined by definite conditions of flow, and, since the pressure at the base of the projectile in free flight will not necessarily be equal to that in the wind tunnel tests, the drag can be calculated for any base pressure.

The fore drag is given in coefficient form by

$$C_{D_F} = C_D + \frac{(P_{mb} - P_s) A}{q A} .$$

In these tests, p_s was taken as the static pressure in test section, p_4.

b) Lift data reduction

The lift force measured by the balance is given from equation (3.2)

$$L_b = 0.010858 \times N_{L_1} + 0.018002 \times N_{L_2} . \qquad (4.10)$$

Similar to the case of drag, the true lift force acting on the model is given by

$$L = (L_b + \Delta L) - L_T = L' - L_T , \qquad (4.11)$$

where ΔL represents the "piston effect" and L_T the remainder of the tare lift force acting on the model support structure. The piston

effect correction for the lift force is

$$\Delta L = -\frac{\pi}{4} d_{ST}^2 \left(P_{bt} - P_{mb} \right)_L \times \sin \alpha_i \ . \qquad (4.12)$$

The lift tare force, L_T, also contains a "piston effect" force, ΔL_T, and it was found in the case of these particular tests that the piston effect of the tare forces was equal to the piston effect of the models, or

$$\Delta L_T = \Delta L \ . \qquad (4.13)$$

So equation (4.11) then becomes, in coefficient form

$$C_L = C_{L_b} - C_{L_T} \ , \qquad (4.14)$$

where C_{L_T} does not include piston effect. The method of determining C_{L_T} is described in Section V.

c) Pitching Moment Data Reduction

The pitching moment about the trunnion axis as measured by the moment balance is

$$M_{o_b} = 0.12422 \times N_{L_2} \ . \qquad (4.15)$$

The true pitching moment about the trunnion axis as exerted by the lift force of the model is again given by

$$M_o = \left(M_{o_b} + \Delta M_o \right) - M_T = M_o' - M_T \ . \qquad (4.16)$$

From figure 4-1 the piston effect correction is given by

$$\Delta M_o = \Delta L \times S = -\frac{\pi}{4} d_{ST}^2 \left(P_{bt} - P_{mb} \right)_L \times \sin \alpha_i \times S \ , \qquad (4.17)$$

where S is the distance from trunnion axis to the center of rotation.

But from equation (4.13), and (4.17),

$$\Delta M_o = S \times \Delta L_T = \Delta M_{o_T} \ ,$$

giving, in coefficient form

$$C_{M_o} = C_{M_{o_b}} - C_{M_T} \ , \tag{4.18}$$

where

$$C_{M_{o_b}} = \frac{M_{o_b}}{\left(\frac{g_c}{P_o}\right) P_o A d}$$

and C_{M_T} is as given in Section V.

d). Determination of Center of Pressure

The distance ℓ from the center of pressure on the model to the balance trunnion axis is determined from

$$\frac{\ell}{d} = \frac{C_{M_o}}{C_L} \ . \tag{4.19}$$

The location of the center of pressure ahead of the model base is

$$\frac{a}{d} = \frac{\ell}{d} - \frac{t}{d} \ , \tag{4.20}$$

where t is the distance from the model base to the trunnion axis. Since $\alpha_i \leq 10^\circ$, no appreciable error has been introduced by the assumption $\cos \alpha_i = 1$.

The pitching moment coefficient referred to the base of the model, C_{M_B}, is then readily determined from

$$C_{M_B} = \frac{a}{d} C_L \ . \tag{4.21}$$

Since $\frac{a}{d}$ is determined from equation (4.20) as the difference of two numbers of the same magnitude, any scatter in C_L or C_{M_o} will be magnified greatly. Therefore, the faired curves of C_L and C_{M_o} versus α_i were used when determining $\frac{\ell}{d}$ from equation (4.19).

Since for $\alpha = 0^o$ both C_{M_o} and C_L approach zero, the values of $\frac{\ell}{d}$ calculated from equation (4.19) for α smaller than 3^o are very inaccurate. Hence, for small angles of attack it is preferable to calculate $\frac{\ell}{d}$ from equation (4.22)

$$\frac{\ell}{d} = \left(\frac{d C_{M_o}}{d\alpha}\right) \Big/ \left(\frac{d C_L}{d\alpha}\right) \qquad (4.22)$$

Equation (4.22) is exactly true only for $C_L = 0$, i.e., $\alpha = 0$, since it is assumed that

$$C_L \times \frac{d}{d\alpha}\left(\frac{\ell}{d}\right) = 0 .$$

e) Angle of Attack Correction

The model support strut deflects elastically as a cantilever beam subjected to the lift load acting on the model. The true angle of attack, α, will then be given by

$$\alpha = \alpha_i + \beta \quad , \qquad (4.23)$$

where

$$\beta = \left(\frac{d\beta}{dL}\right)_L \times L \, . \qquad (4.24)$$

The value of $\left(\frac{d\beta}{dL}\right)_L$ is given in figure 4-2 as a function of the center of pressure position, "a". The curve of $\frac{d\beta}{dL}$ versus "a" was determined[1a] by a direct static calibration of the angular deflection of the cantilever end of the model support strut.

f) Calculation of Reynold's Number, R, [illegible]

The Reynold's Number, R, is defined as,

$$R = \frac{\rho u C}{\mu} , \tag{4.25}$$

where μ and ρ are the viscosity and density of the test section air, respectively, and u is the relative velocity between model and air stream. For projectile model tests the characteristic length, C, is defined as the overall length of the model. The product $\frac{\rho u}{\mu}$ is a function of Mach Number, M, and supply pressure, P_o, only, so that equation (4.25) may be written as

$$R = 3.62 \times 10^5 \times P_o \times C \times f(M). \tag{4.26}$$

where P_o is expressed in atmospheres, C in inches, and the function f(M) is given in figure 4-3, $T_o = 100^\circ$ F.

1a Puckett, A. E., and Schamberg, R.; Final Report - GALCIT Supersonic Wind Tunnel Projectile Tests Contract W-101 ORD-1312 (741) , page 31.

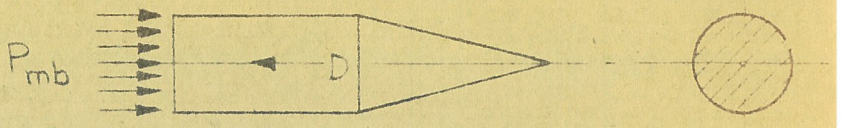

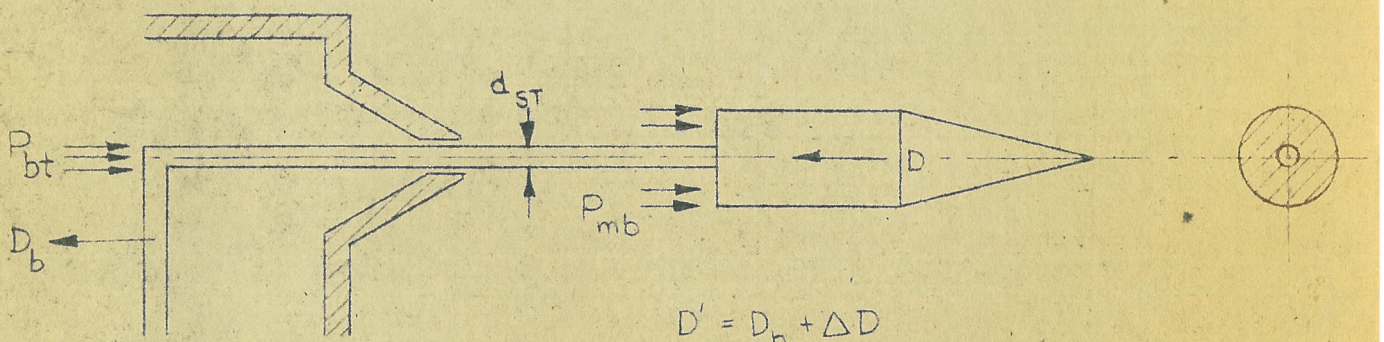

$$D' = D_b + \Delta D$$

$$\Delta D = \frac{\pi}{4} d_{ST}^{\,2} (P_{bt} - P_{mb})$$

FIG. 4-1

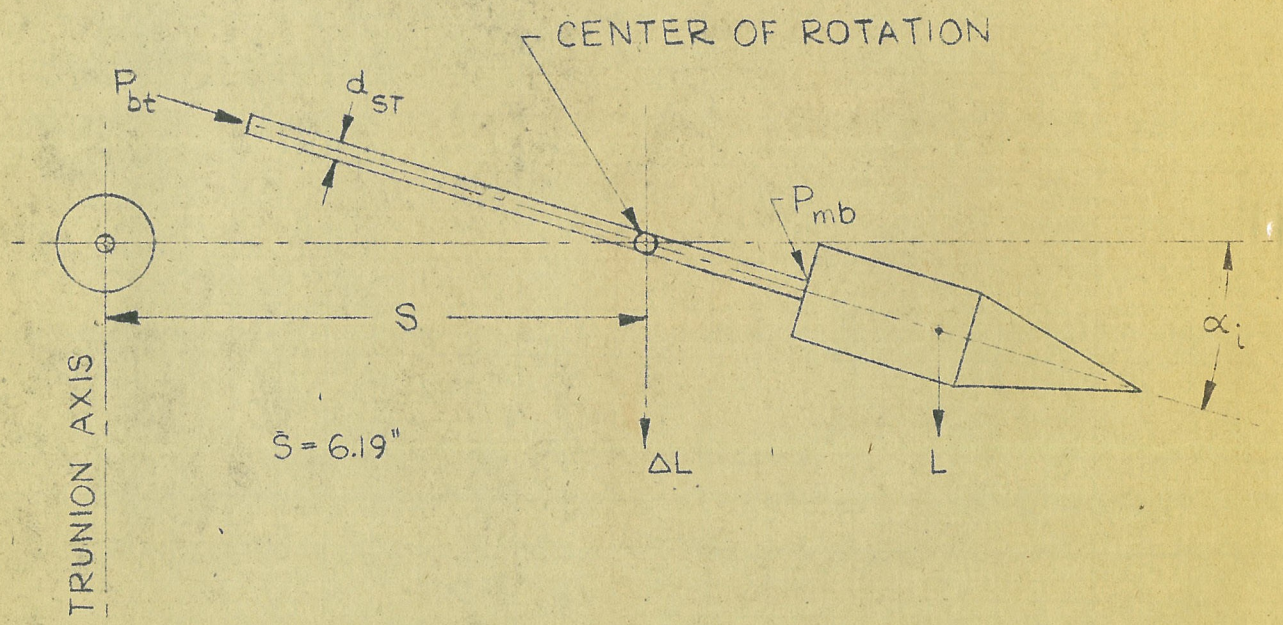

FIG. 4-1A

ANGLE OF ATTACK CORRECTION FOR STRUT DEFLECTION

(STRUT NO. 2)

$$\alpha = \alpha_i + \theta$$

$$\theta = \left(\frac{d\beta}{dL}\right) \times L_b$$

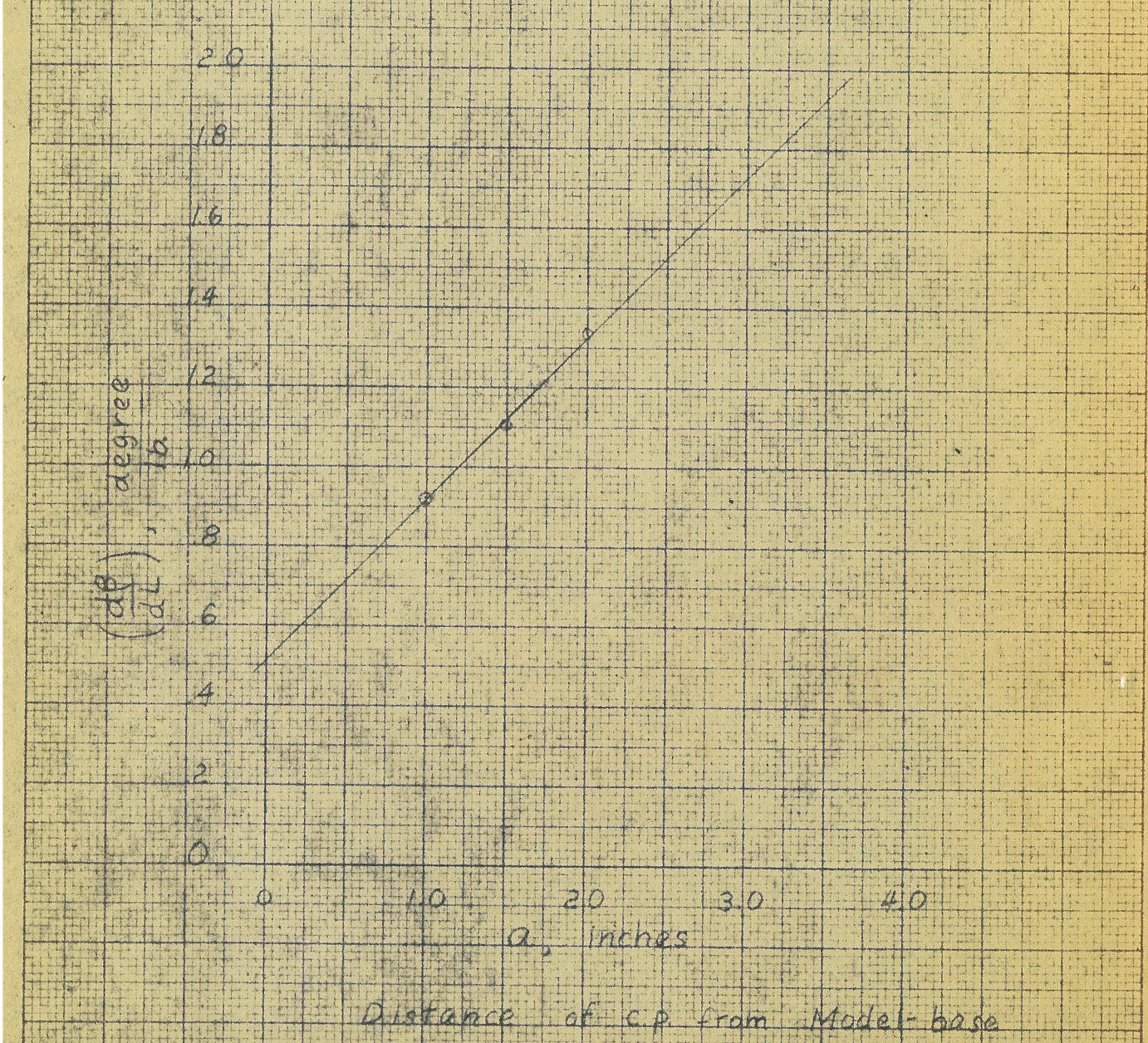

Fig. 4-2

R.S.
3-8-46

REYNOLDS NUMBER VS MACH NUMBER

$$R = 3.62 \times 10^5 \, P_0 \cdot C \cdot f(M)$$

P_0 in atmospheres
C in inches

Based on $T_0 = 100°F$
$\gamma = 1.404$

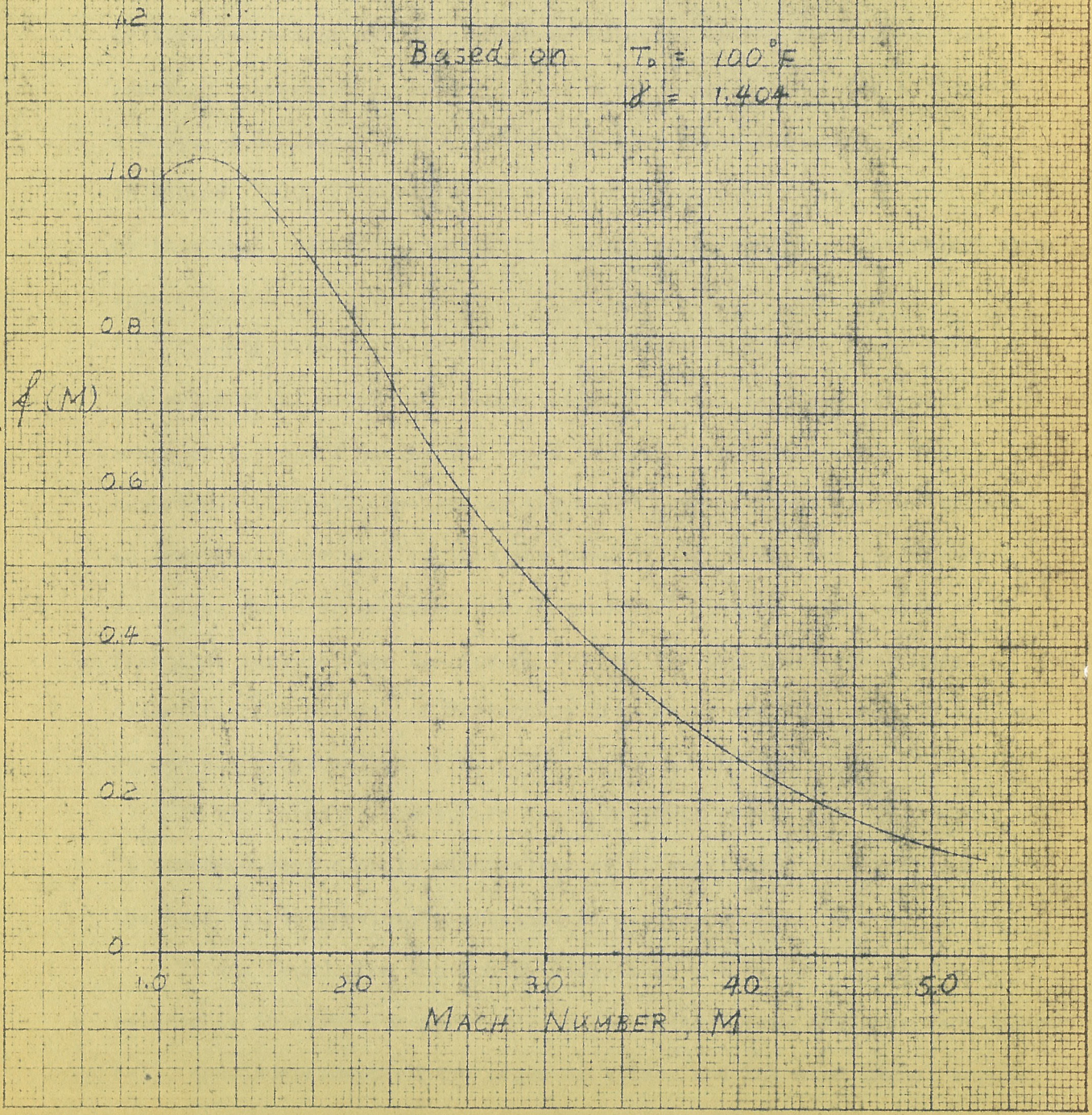

Fig. 4-3

R.S.
3-9-46

V. Determination of the Tare Forces

At supersonic speeds the convergent wake of a sphere closely resembles that of cylindrical projectiles. From the symmetry of the sphere, its lift must be zero and its drag constant for all angles of attack. Therefore, if a sphere of diameter d_1 be tested by means of the routine testing procedure described in Section IV the resulting values of lift and moment may be assumed to be equal to the tare forces, L_T and M_{OT}, respectively, acting on the model support strut for a diameter $d = d_1$. A Schlieren photograph of the flow about the sphere is shown in figure 7-10. The variation of D_T with angle of attack is also given by this test, although the absolute value of D_T cannot be determined from sphere tests.

The absolute value of D_T is usually determined from tests in which the cylindrical model is attached rigidly to the test section wall by means of a support having the cross section of a thin, double-wedge, supersonic airfoil. The end of the model support strut is free inside an oversized hole drilled into the base of the model, and the standard technique for drag measurements (Section IV) is used. The value of D' from this test is then D_T for $\alpha_i = 0$ and for the appropriate model diameter. The results of the sphere drag tests are then used to evaluate D_T for all other values of x_1.

It was found in the sphere tests for this report that the values of C_D compared very closely with values of C_D previously obtained, and so the tare values previously obtained were used for this report.

It was found from the sphere tests that the tare force on the L_1 balance is inversely proportional to the balance tank pressure (see figure 5-1), and independent of the angle of attack and the wind tunnel supply

pressure, p_o. The tare force on the L_2 balance was found to be independent of the balance tank pressure and p_o, but was found to vary with the angle of attack as shown in figure 5-2.

LIFT TARES

L_1

L_1 INDEPENDENT OF ANGLE OF ATTACK AND P_0

VALUE FROM THIS CURVE TO BE SUBTRACTED FROM VALUE OF RUN

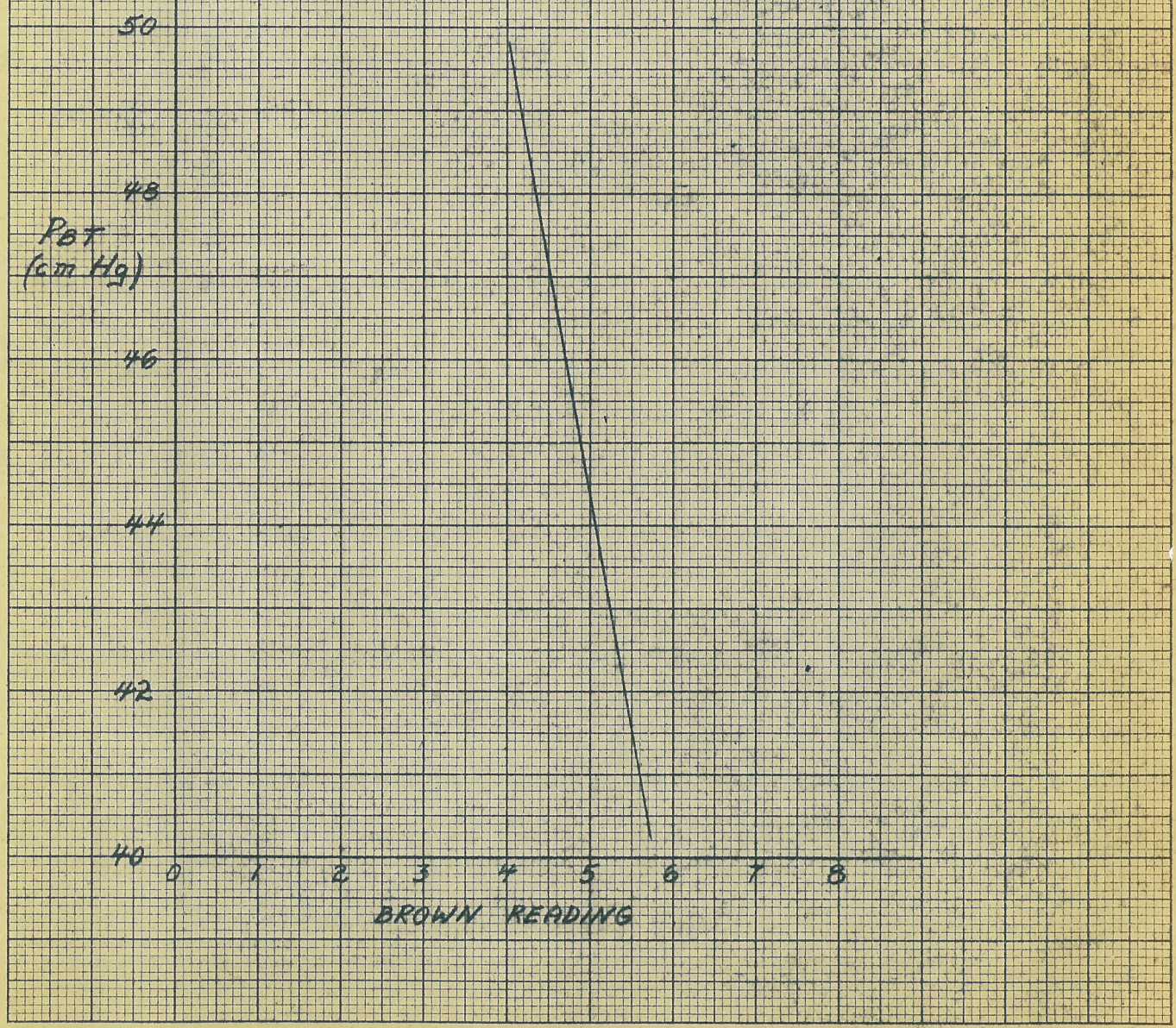

FIG 5-1

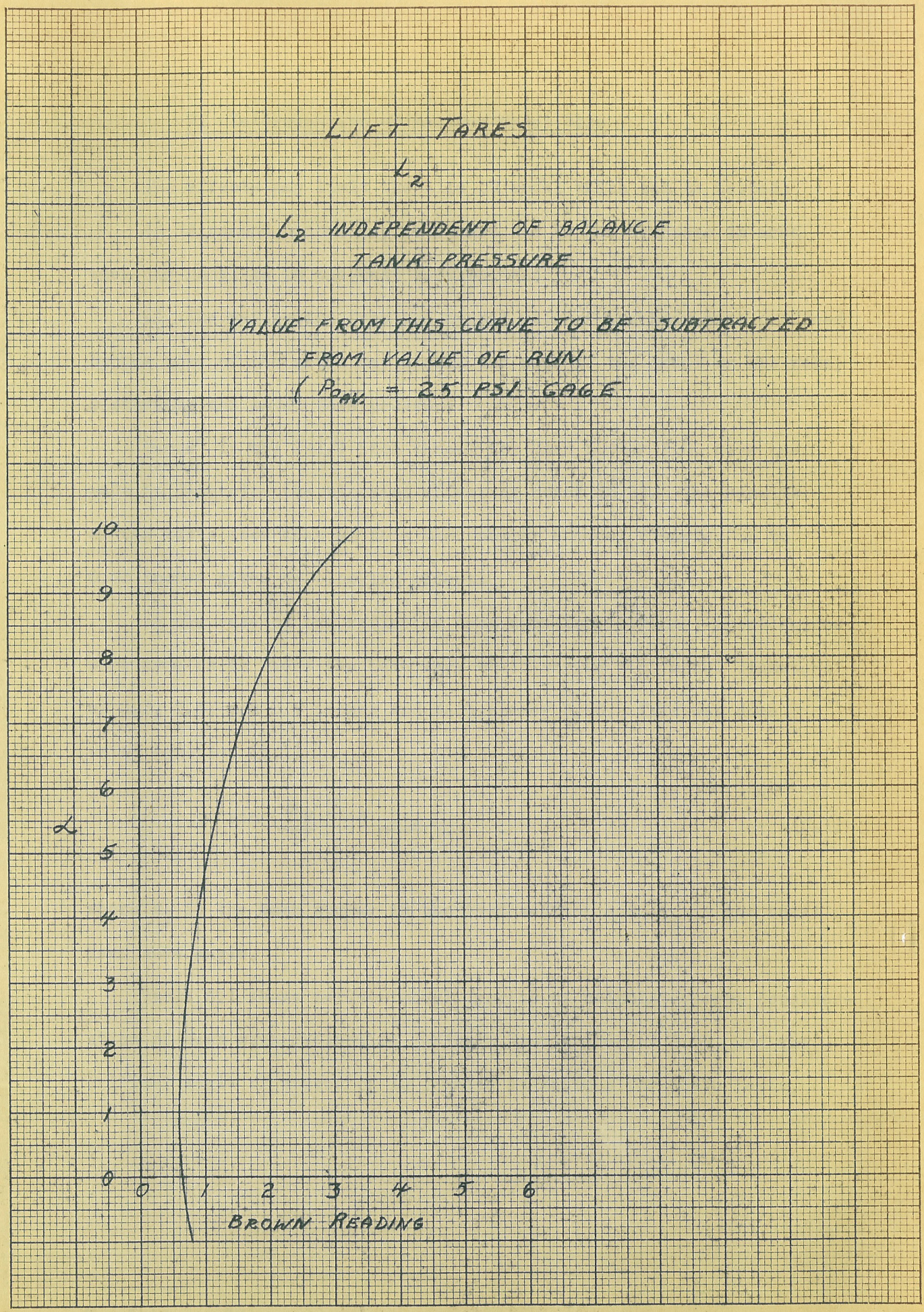
LIFT TARES
L_2
L_2 INDEPENDENT OF BALANCE TANK PRESSURE
VALUE FROM THIS CURVE TO BE SUBTRACTED FROM VALUE OF RUN
(P_{TANK} = 25 PSI GAGE
L
10
9
8
7
6
5
4
3
2
1
0
0
1
2
3
4
5
6
BROWN READING

FIG 5-2

VI Determination of Maximum Model Size

Two effects may limit the size of model which can be tested:

1) A second throat may be formed due to the decrease in area when the model is in the test section, and

2) The reflection from the tunnel wall of the head wave produced by the nose of the model may strike the rear of the model or its wake, disturbing the model base pressure.

Tests[2] in the 2-1/2 inch throat for Mach number 3.06 have been made to determine the blocking effect as noted in 1). The results of the tests show that at this Mach number a model diameter up to 0.68 inches gives no blocking effect.

In the case of the reflected head wave interference, calculations were made as to where the head wave would strike with model diameters of 0.3, 0.4, and 0.5 inches and Mach number 3.06. This was done using equation (6.1)

$$\sin \frac{\alpha_H}{2} = \frac{1}{M_T} \qquad (6.1)$$

where M_T is the Mach number in the test section and α_H is the total head wave angle.

Table 6.1 shows maximum model lengths as calculated from consideration of head wave reflection, using a Mach number of 3.06, and the critical angle of attack of 10°, which is maximum for these tests.

---

2. Ibid, p. 36

Model Diameter (inches)	Model scale length	Critical length M = 3.06 $\alpha = 10^{\circ}$
0.3	4.60	3.9
0.4	6.06	3.8
0.5	7.25	3.6

TABLE 6.1

Critical Length Tabulations Due to Head Wave Reflection

However, the length of test section in which smooth supersonic flow at constant Mach number occurs was found to be the factor determining model length in this case. The base of the model had to be placed sufficiently upstream on the support strut to avoid interference between the wake and the windshield, and the nose of the model could not be placed upstream of the test section. These factors determined a maximum model length of 3.25 inches. For the 0.3 inch diameter model used in these tests, thelength of the cylindrical section had to be reduced 1.35 inches. It was thought that this reduction of model length would not affect the forces appreciably.

Models "A" and "B" are shown in Figures 6-1 and 6-2, respectively.

FIG 6.1

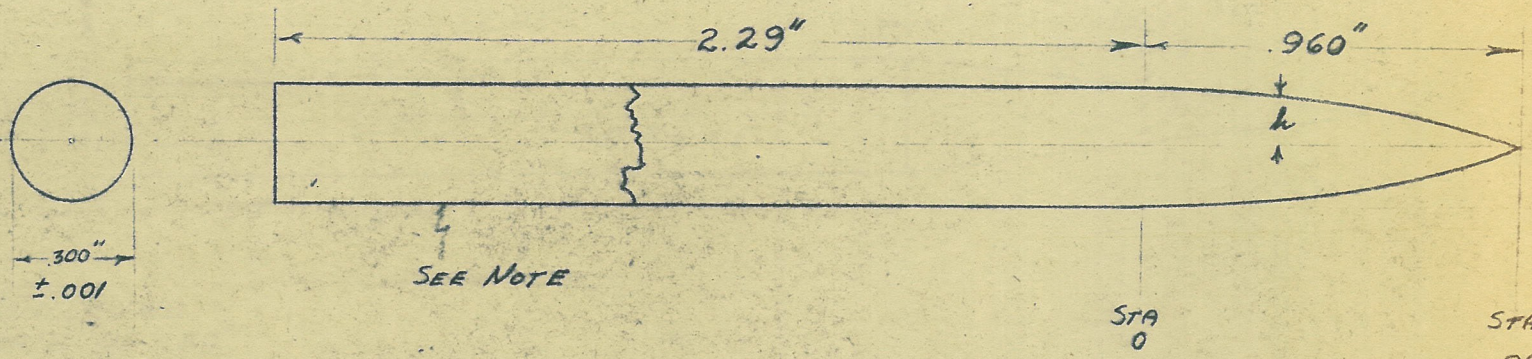

NOTE: 1) BASE OF MODEL TO BE IDENTICAL WITH DRAWING 4-258-303 (FIG)

2) EQUATION OF NOSE IS $h = .15\left[1 - \left(\frac{\text{STA. No.}}{.96}\right)^2\right]$

3) "h" VALUES TO BE HELD TO ±.002".

STA. No.	0	.1"	.2"	.3"	.4"	.5"	.6"	.7"	.8"	.9"	.96"
h	.150"	.148"	.144"	.135"	.124"	.109"	.091"	.070"	.046"	.018"	0

MATERIAL	FINISH	HEAT TREAT	DRAFTSMAN	CHECKED	APPROVED	ENGINEER	TOLERANCES ± .010 OR 1/64 UNLESS OTHERWISE NOTED
BRASS	SMOOTH MACHINE & POLISH	—	N.S.		GEP		SCALE ~ DOUBLE SIZE
							28 FEB., 1947

GUGGENHEIM AERONAUTICAL LABORATORY
CALIFORNIA INSTITUTE OF TECHNOLOGY

NAME: WIND TUNNEL MODEL "A"

DRAWING NO.: 4-258-304

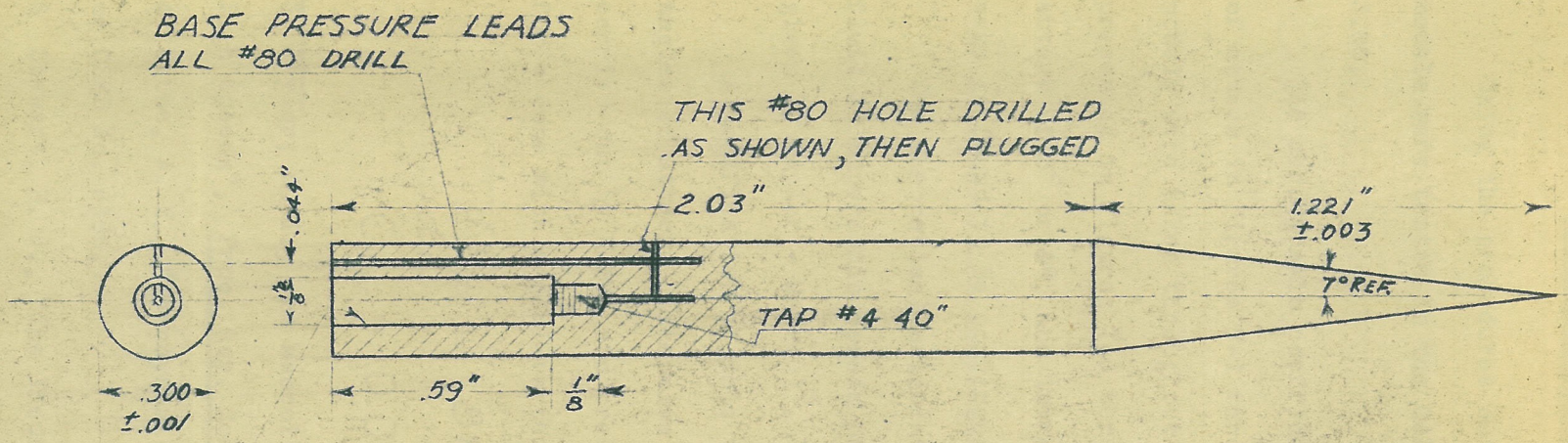

BRASS	SMOOTH MACHINE & POLISH	—					TOLERANCES ± .010 OR 1/64 UNLESS OTHERWISE NOTED
			MWF		AEP		SCALE ~ DOUBLE SIZE
MATERIAL	FINISH	HEAT TREAT	DRAFTSMAN	CHECKED	APPROVED	ENGINEER	28 FEB. 1947
GUGGENHEIM AERONAUTICAL LABORATORY CALIFORNIA INSTITUTE OF TECHNOLOGY			WIND TUNNEL MODEL "B"				4-258-303
			NAME				DRAWING NO.

Fig. 6.2

VII. Test Results and Analysis

Using the procedures outlined in earlier sections, two projectile models were tested in the GALCIT supersonic wind tunnel at Mach Number 3.06.

The aerodynamic coefficients have been plotted as a function of angle of attack in figures 7-1 through 7-4. Schlieren photographs of both models were taken throughout the range of angles of attack. They are presented in figures 7-5 through 7-17. Separation occured at an angle of attack of 3° or 4°, and increased with increasing angle of attack. The wake is found to be convergent at all times.

The theoretical calculations of the non-viscous flow of a compressible fluid at supersonic speeds past a cone at zero angle of attack was first given by Taylor - Maccoll[3].

A modification of this theory was given by Stone[4] for cones at small angles of attack. Extensive numerical integrations for these theories were carried out by Kopal and presented by Stewart[5]. These calculations give for a cone with a semi-vertex angle of 7°.

$$\frac{d C_L}{d \alpha} = 1.810$$

$$C_{D_W} = 0.0488$$

3 Taylor, G. I., and Maccoll, J. W., "The Air Pressure on a Cone Moving at High Speeds", Proc. Ray. Soc., A, 139:278, 1933.

4 Stone, A. H., "Aerodynamics of a Slightly Yawing Cone", NDRC No. A356 or OSRD No. 6386.

5 Stewart, H. J., "The Theoretical Lift and Drag of Cones at Supersonic Speeds", ORDCIT Project Memorandum No. 4-14, November 18, 1946.

where C_{D_W} = wave drag.

From the tests on the model with the conical nose, the following values were obtained

$$\frac{dC_L}{d\alpha} = 1.9$$

$$C_{D_F} = .10$$

where C_{D_F} = wave drag + skin friction.

So, for this model, the skin friction drag coefficient, C_{D_τ}, would be equal to the experimental drag coefficient minus the theoretical wave drag

or, $$C_{D_\tau} = C_{D_F} - C_{D_W} = 0.051$$

now, $$C_{D_\tau} = \frac{\text{wetted area}}{\text{cross-sectional area}} \times C_f$$

where C_f is the coefficient of skin friction.

Solving this for C_f, it is found that

$$C_f = .00145.$$

This value appears to be quite reasonable for this method of determination.

It is to be noted that the slope of the lift curve, $\frac{dC_L}{d\alpha}$, as obtained from these tests, is not constant, as predicted by the linear

theory. At high angles of attack, part of this non-linearity of the lift curve is probably due to the separation off the upper surface which was first noted at angles of attack between 3° and 4°. However, at very low angles of attack, no separation was noted. The non-linearity in this region may be explained by the small perturbation theory.

The small perturbation theory for supersonic flow gives

$$\frac{dC_L}{d\alpha} = A f_1\left(\frac{1}{\sqrt{M^2-1}}\right) + B f_2(M)\alpha + \cdots\cdots ,$$

where A and B are constants and f_1 and f_2 are functions of the Mach number only.

For values of M near 1, and α small, the second term becomes negligible as compared to the first term, and the theory may be linearized. However, for high values of Mach Number, the second term becomes increasingly important. It is considered that the Mach Number at which these tests were conducted is sufficiently high to show the effect of the second order term.

MODEL A

MACH NUMBER = 3.06
REYNOLDS NUMBER = 1.4×10^6

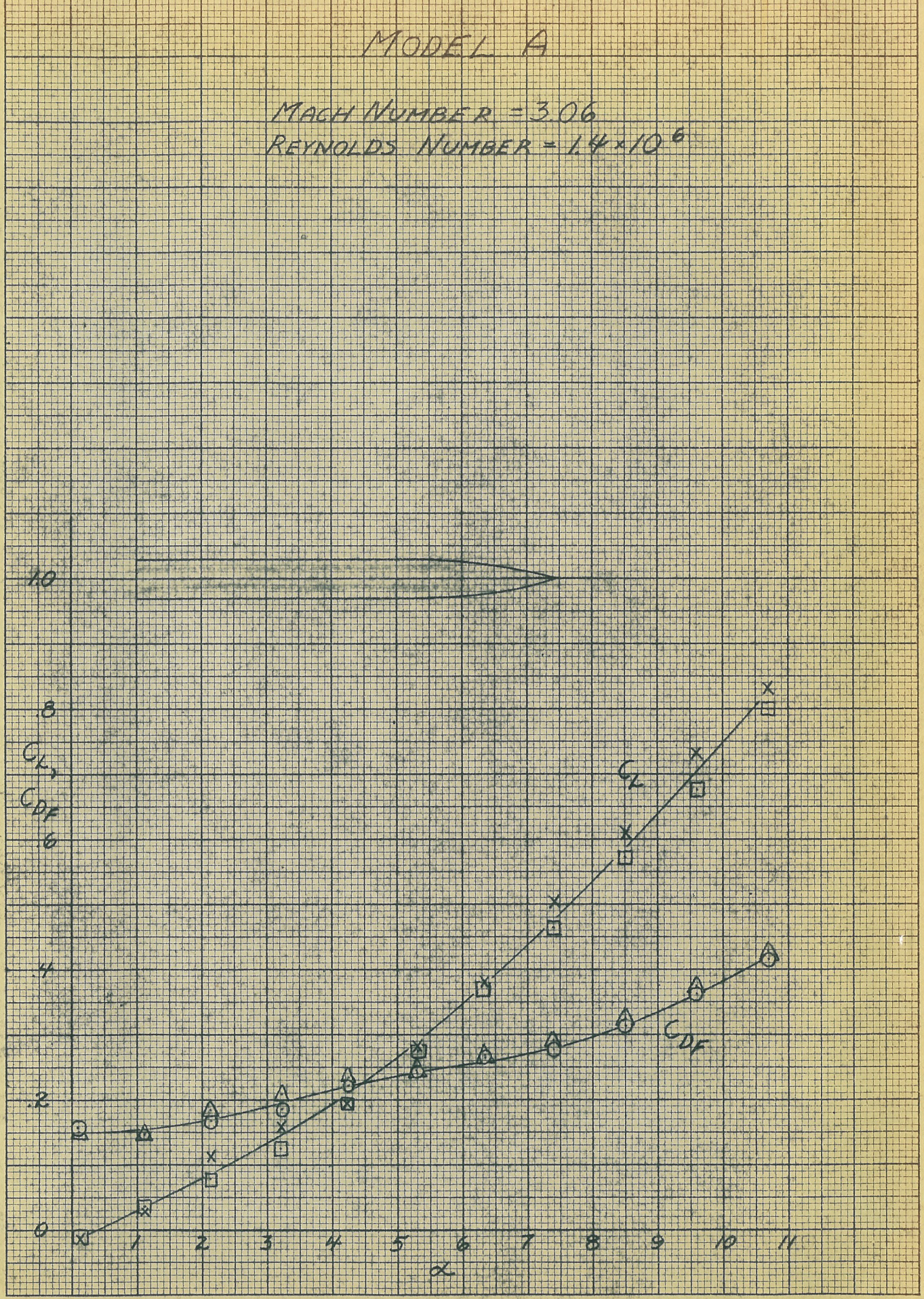

Fig 7-1

MODEL B

MACH NUMBER = 3.06
REYNOLDS NUMBER = 1.4×10^6

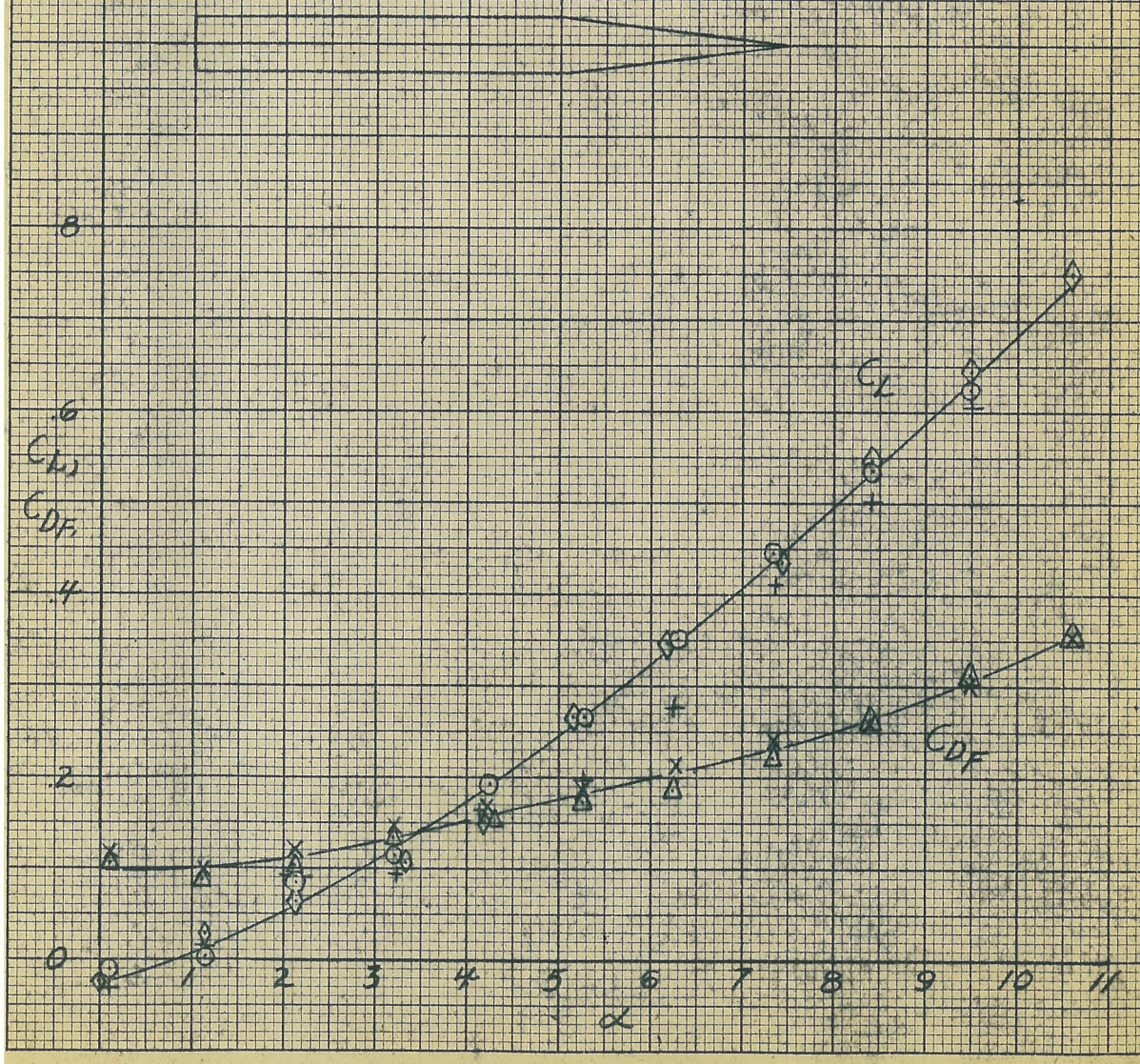

FIG 7-2

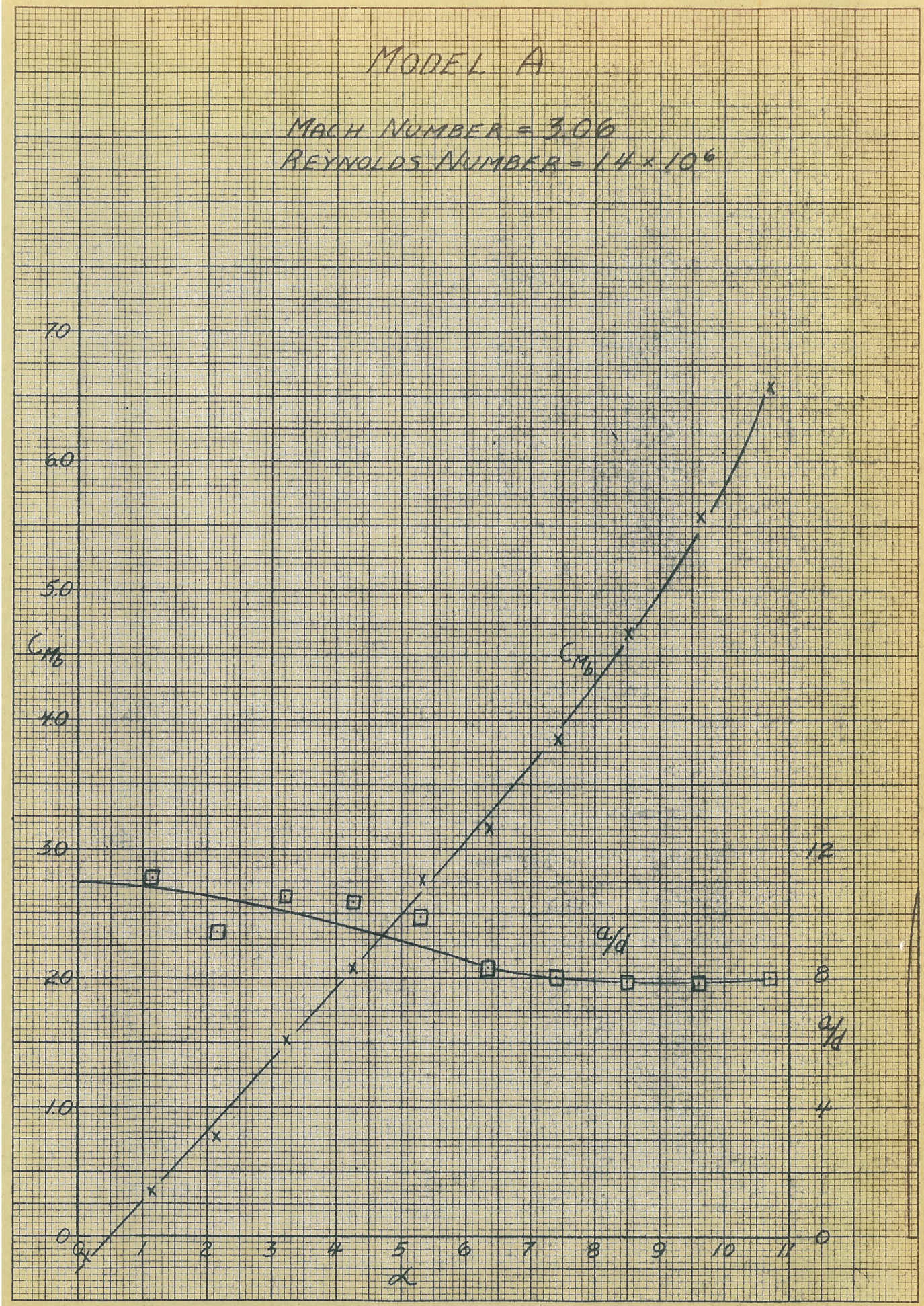
MODEL A
MACH NUMBER = 3.06
REYNOLDS NUMBER = 1.4 × 10⁶
7.0
6.0
5.0
C_{M_b}
4.0
3.0
2.0
1.0
0
C_{M_b}
C_{M_b}
a/d
12
8
4
0
a/d
0
1
2
3
4
5
6
7
8
9
10
11
α

FIG 7-3

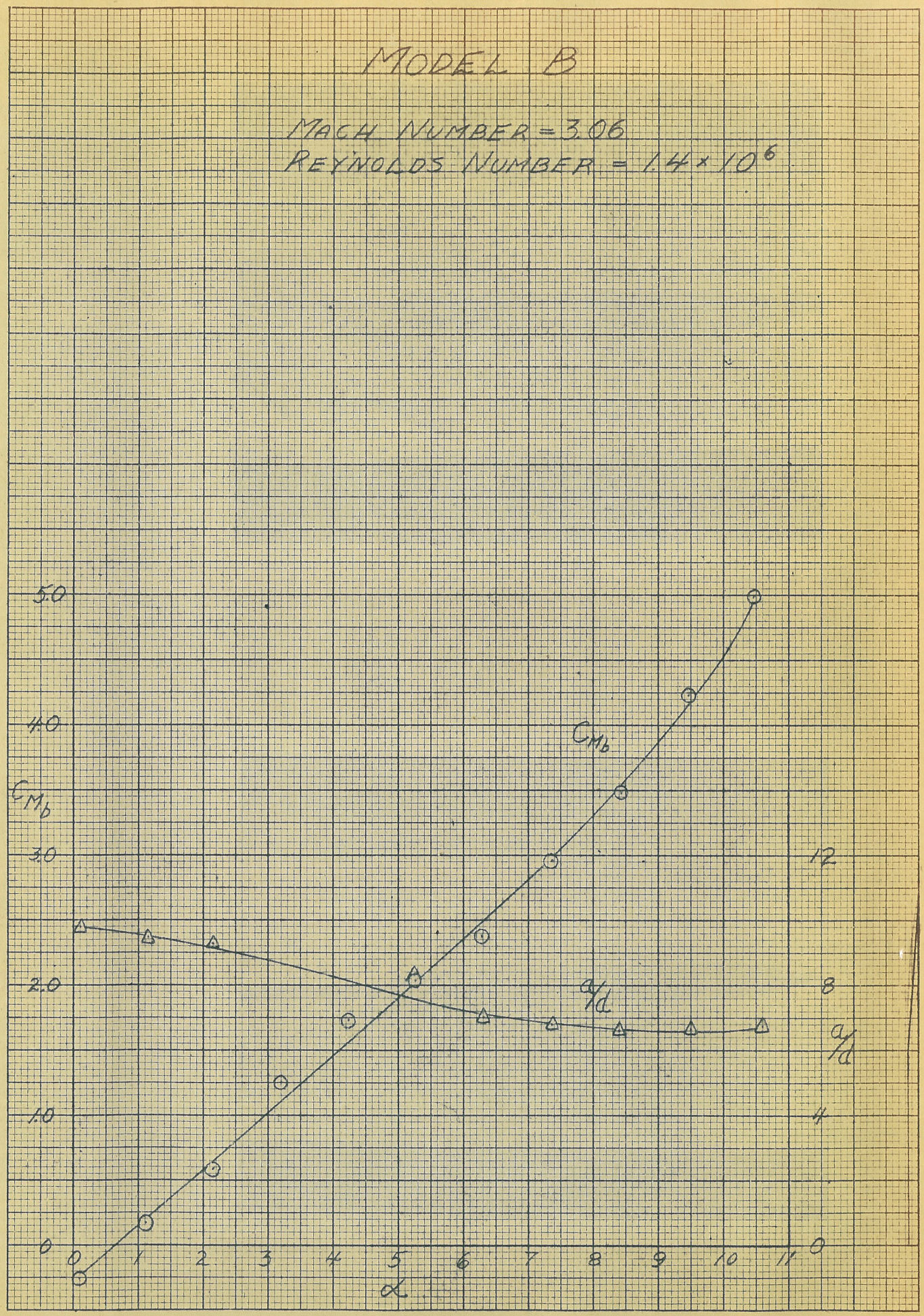
MODEL B
MACH NUMBER = 3.06
REYNOLDS NUMBER = 1.4 × 10^6
5.0
4.0
3.0
2.0
1.0
0
C_{M_b}
12
8
4
0
a/d
0 1 2 3 4 5 6 7 8 9 10 11
α

FIG 7-4

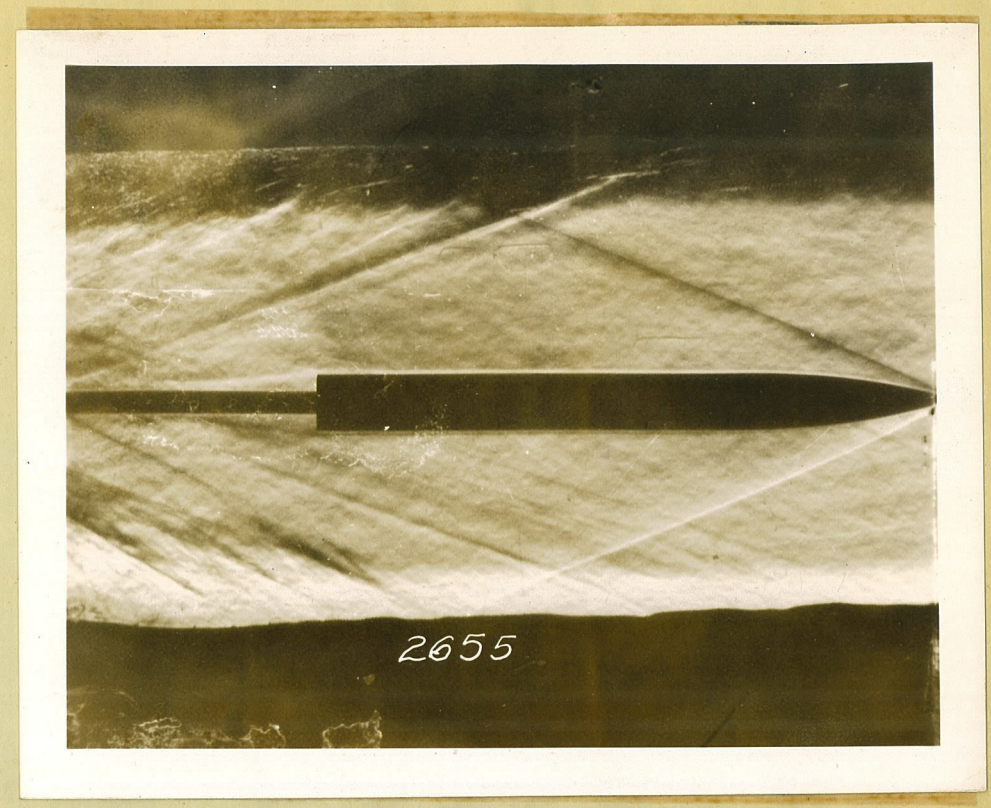

$\alpha = 0°$

Figure 7-5

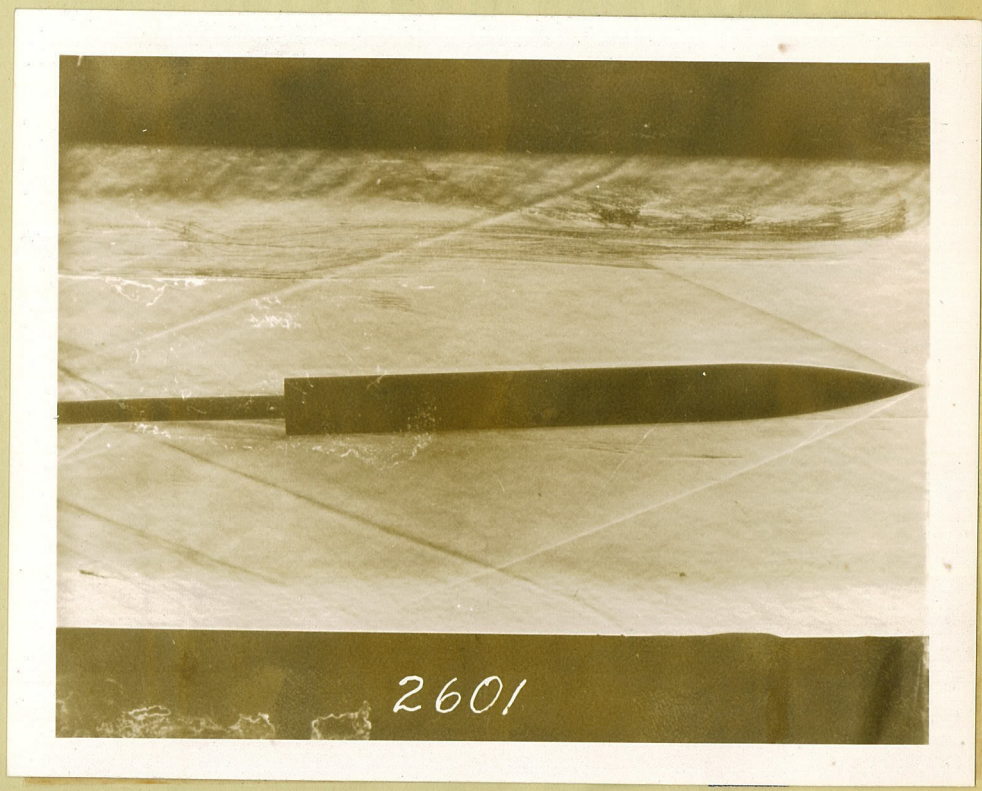

$\alpha = 3°$

Figure 7-6

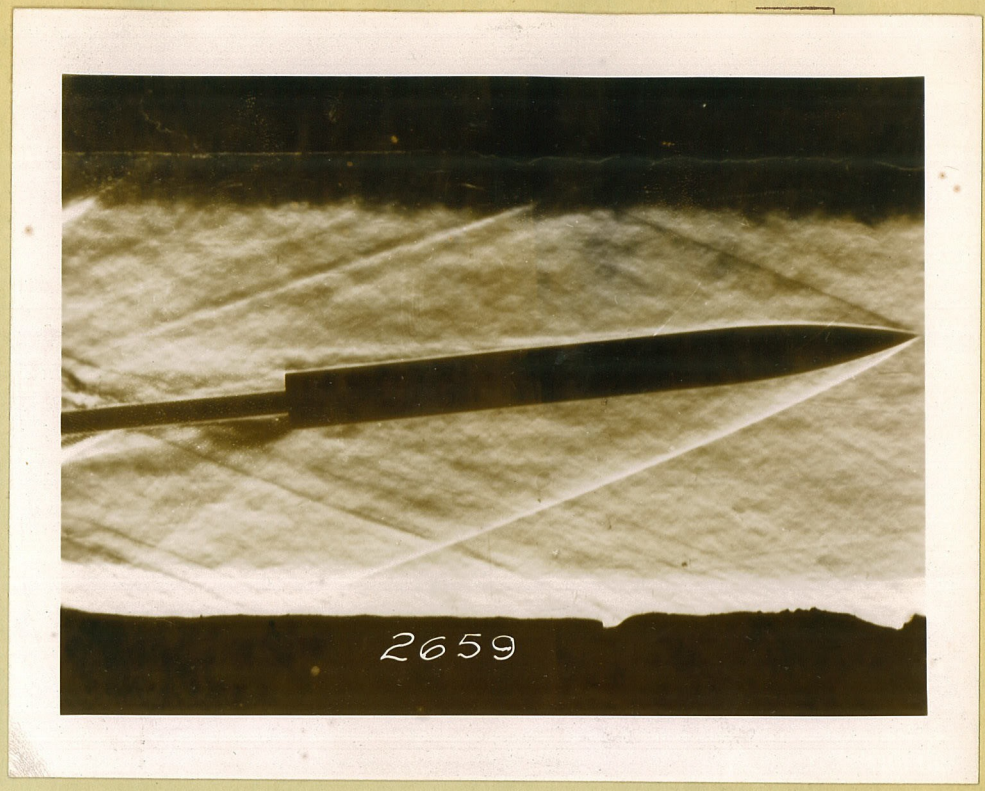

$\alpha = 7^\circ$

Figure 7-7

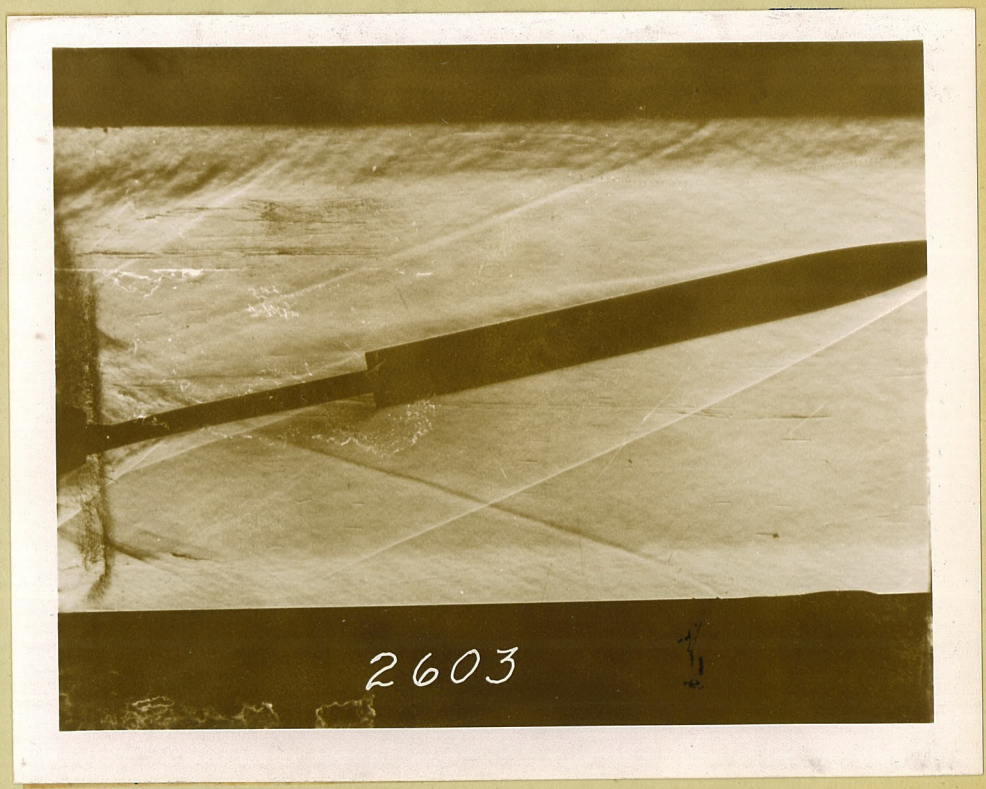

$\alpha = 10^\circ$

Figure 7-8

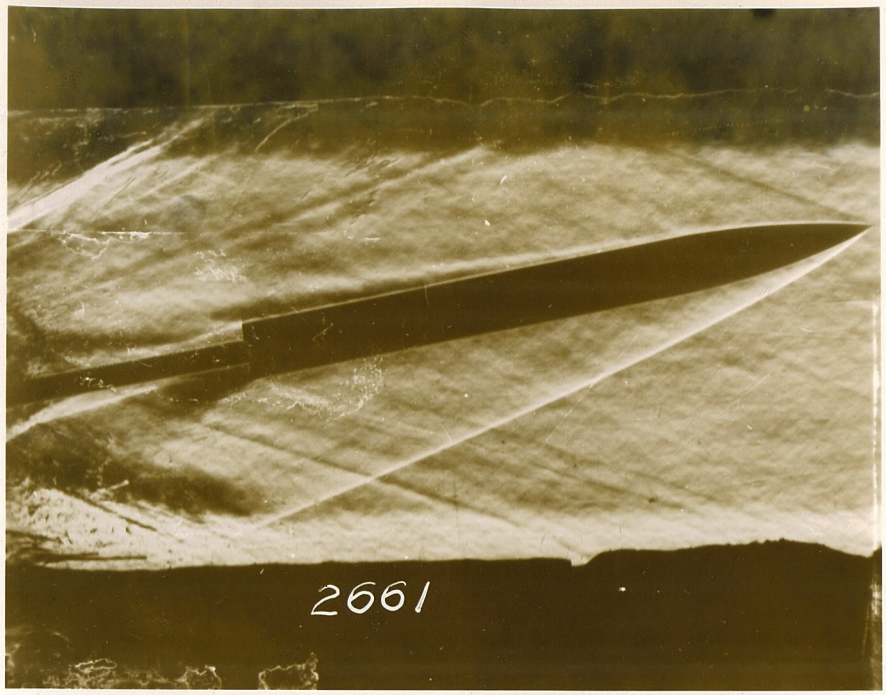

$\alpha = 10^\circ$

Figure 7-9

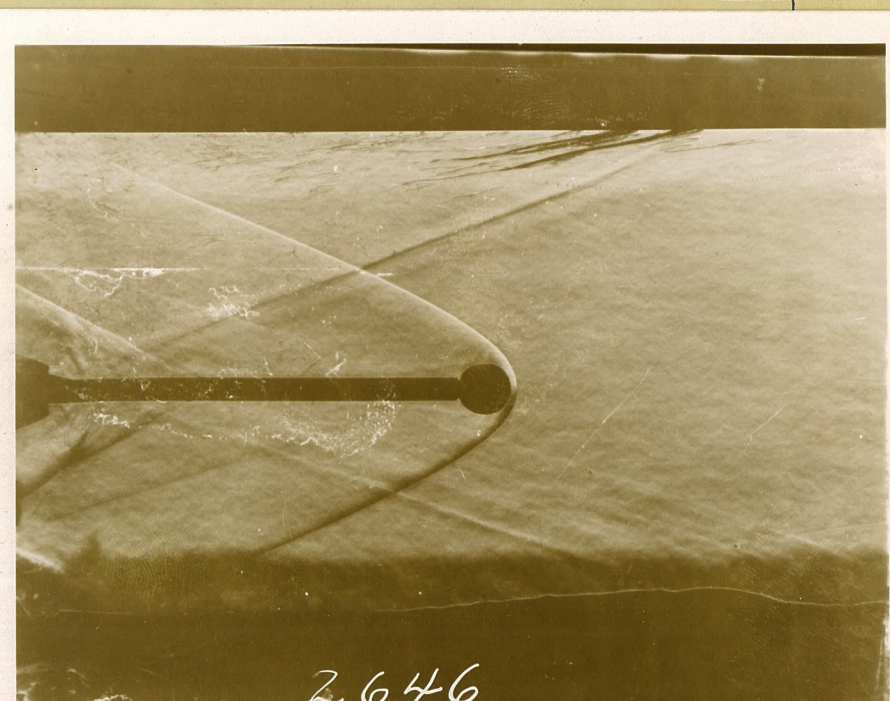

$\alpha = 0^\circ$

Figure 7-10

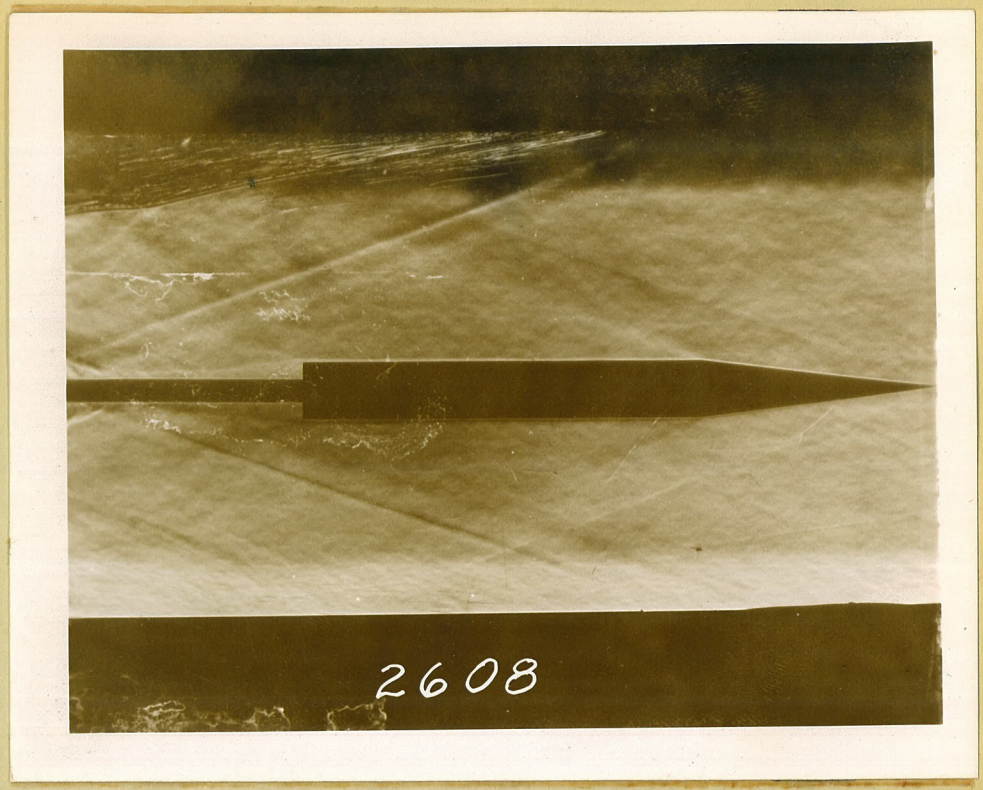

$\alpha = 0^\circ$

Figure 7-11

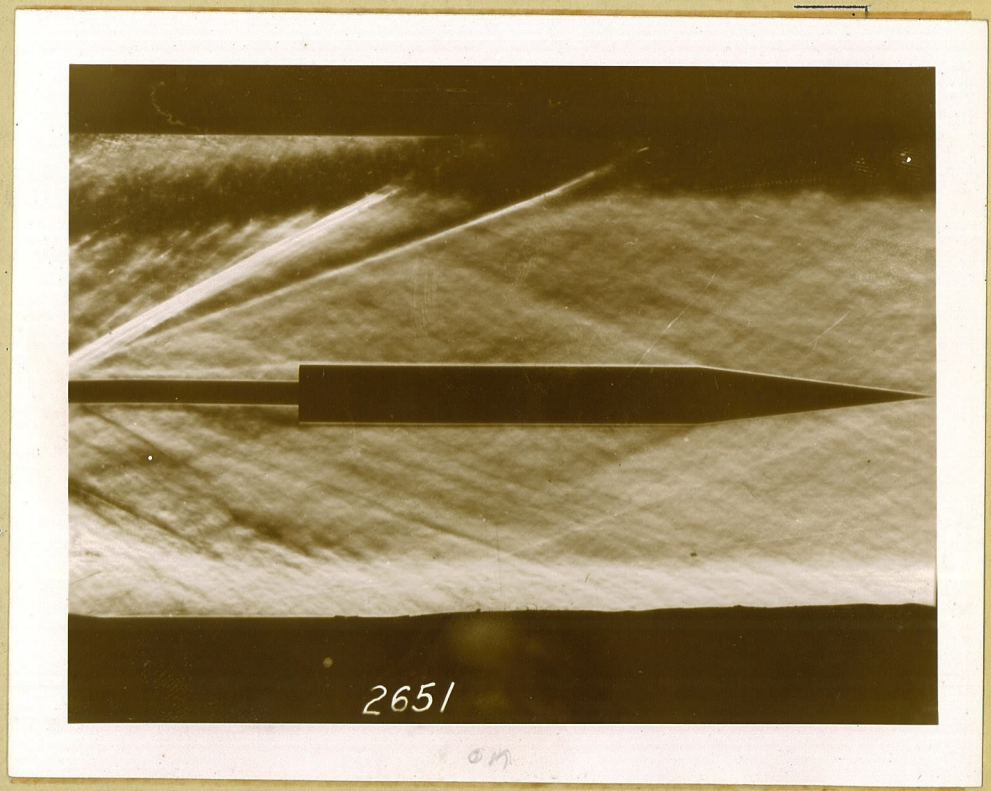

$\alpha = 0^\circ$

Figure 7-12

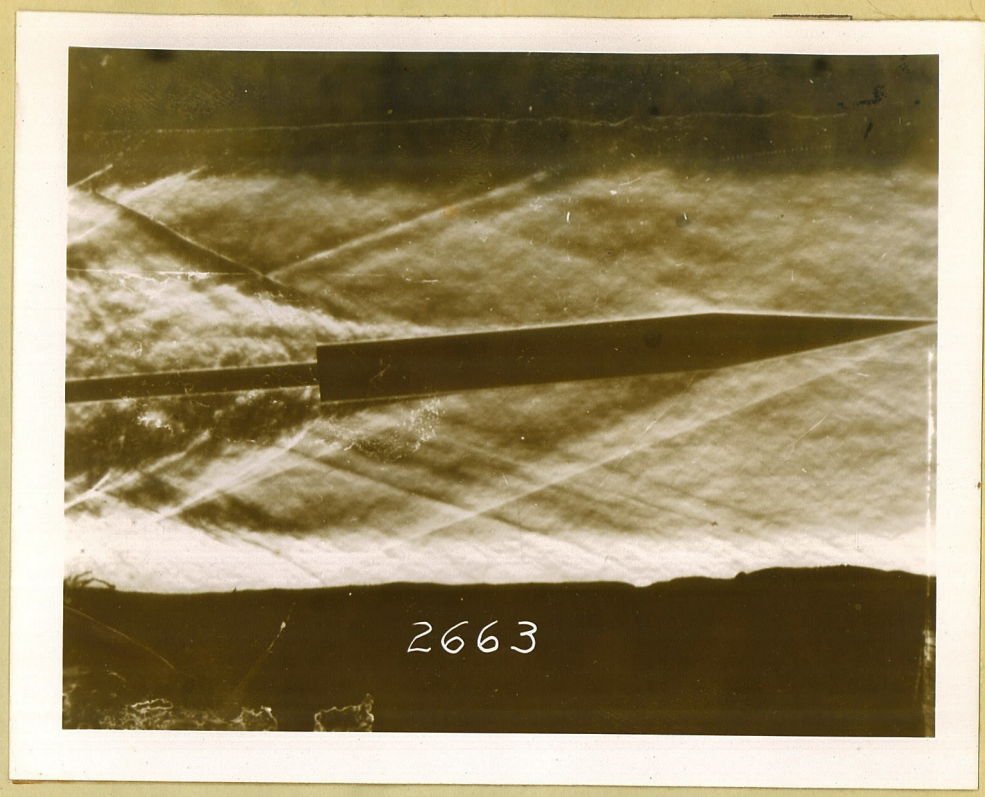

$\alpha = 5^\circ$

Figure 7-13

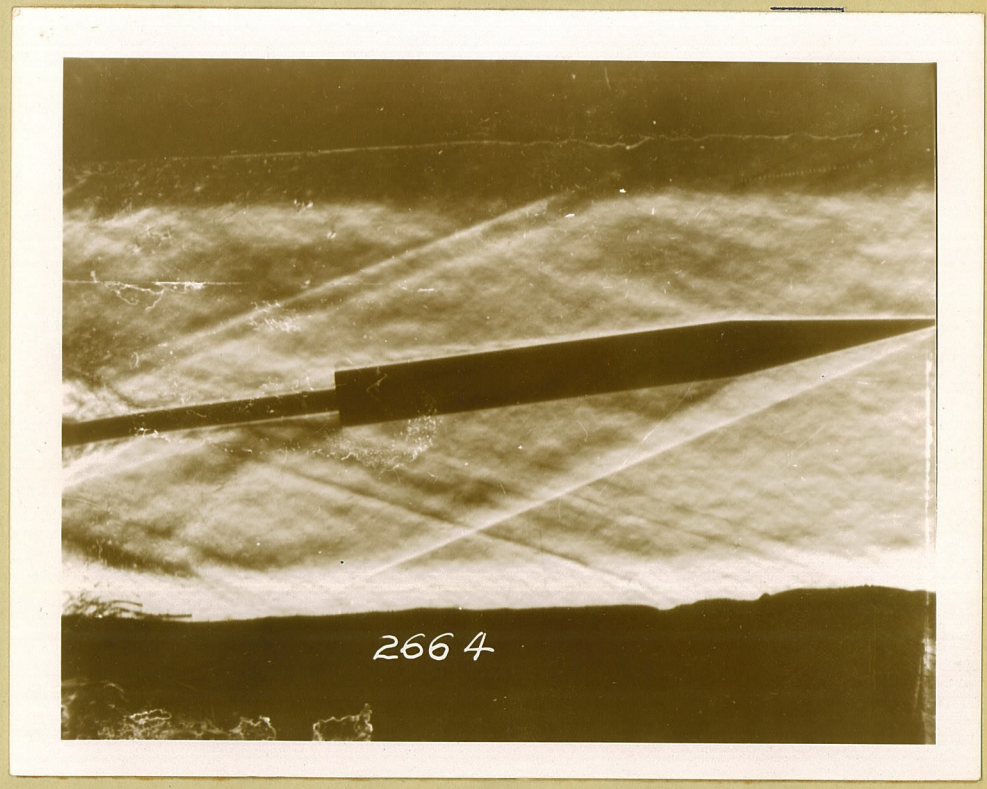

$\alpha = 7^\circ$

Figure 7-14

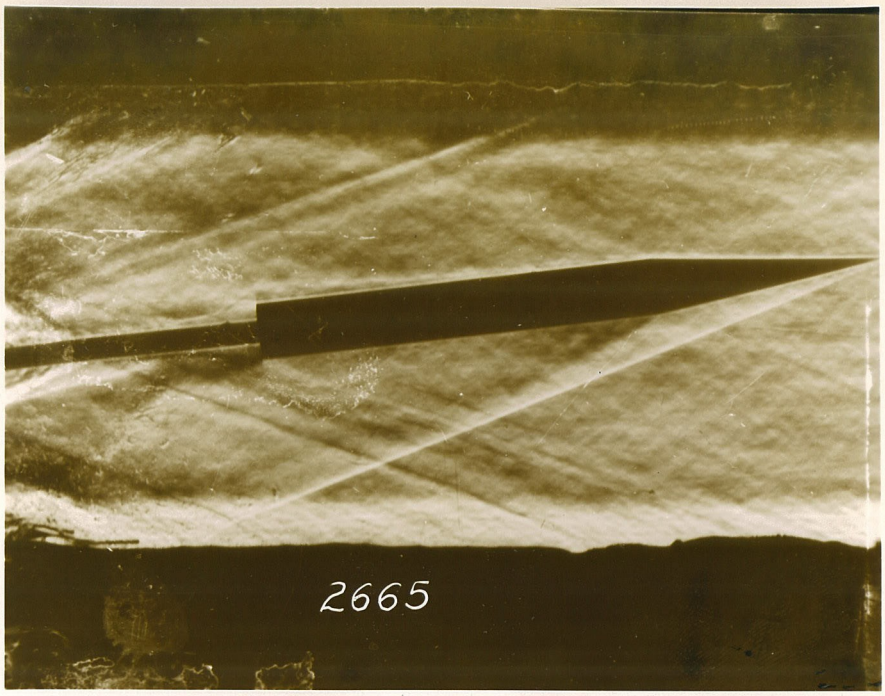

$\alpha = 8°$

Figure 7-15

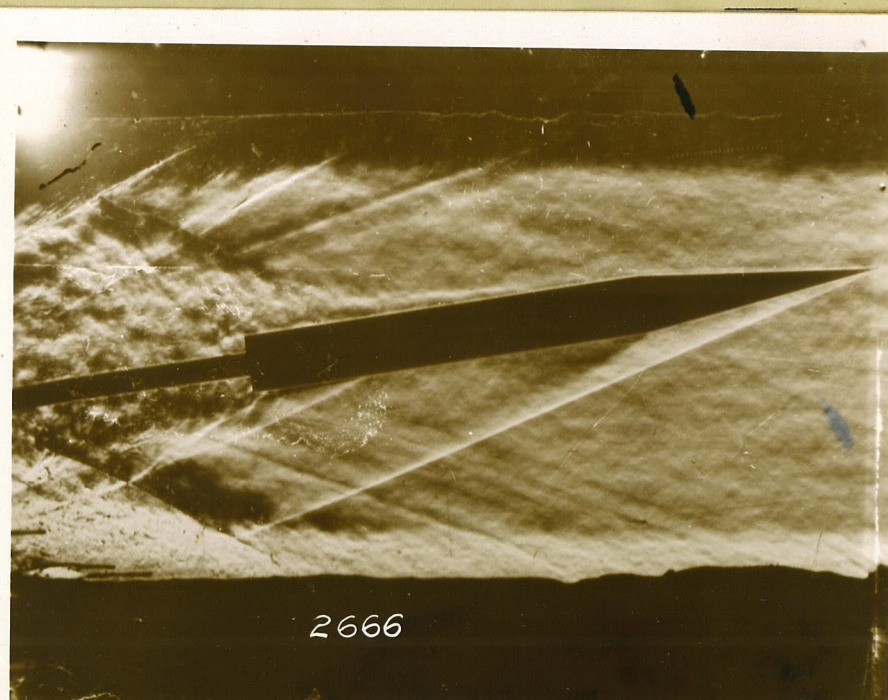

$\alpha = 10°$

Figure 7-16

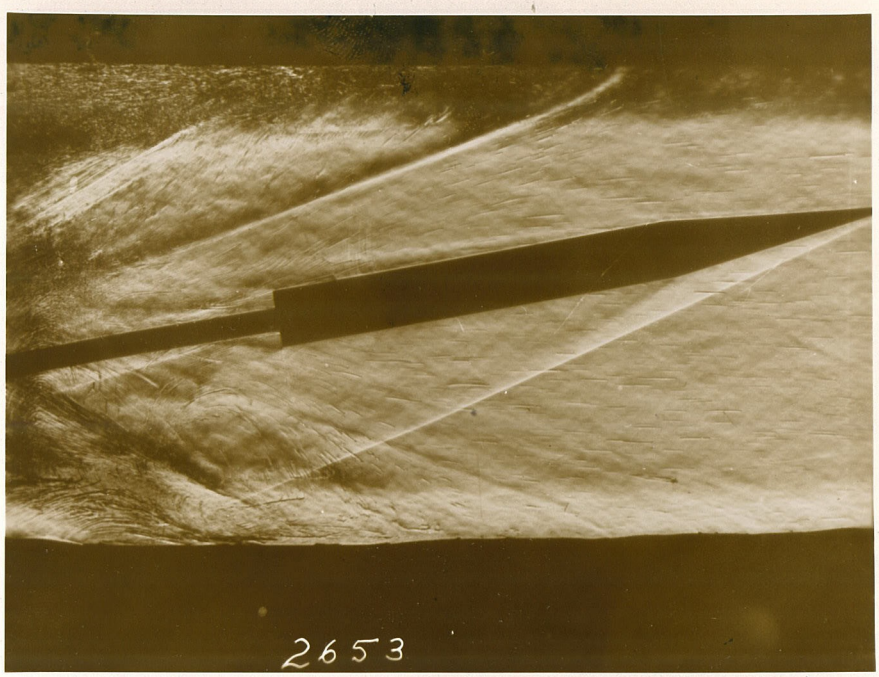

$\alpha = 10^\circ$

Figure 7-17

$\alpha =$

Figure